NMPC Project 03-9425
MPM-USE-293216

FINAL REPORT

entitled

ELASTIC-PLASTIC FRACTURE MECHANICS ASSESSMENT OF NINE MILE POINT UNIT 1 BELTLINE PLATES FOR SERVICE LEVEL C AND D LOADINGS

MPM Research & Consulting

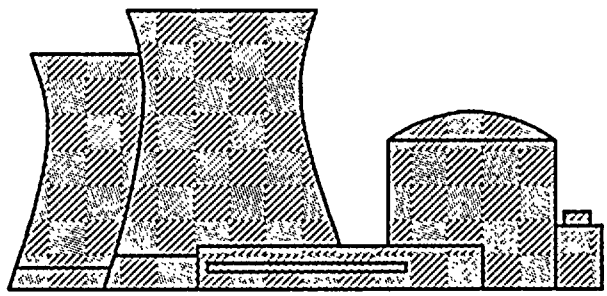

February 22, 1993

Table of Contents

1.0 Introduction

Nuclear reactor pressure vessel materials must be tested and evaluated to ensure that they are safe in terms of both brittle and ductile fracture under normal operation and during design basis transients. With regard to ductile fracture protection, Appendix G to 10 CFR 50 prescribes a screening criterion of 50 ft-lbs. If any beltline materials are expected to exhibit Charpy Upper Shelf Energy (USE) (T-L orientation) levels below 50 ft-lbs, then additional analyses must be performed to ensure continued safe operation. The Draft ASME Appendix X [ASME92] was developed to assist licensees in performing elastic-plastic fracture mechanics evaluations for beltline materials with low upper shelf energies. This report documents application of the draft Appendix X calculative procedures and criteria to two Nine Mile Point Unit 1 (NMP-1) beltline plates for Service Level C and D loadings.

The NMP-1 beltline materials were evaluated to determine whether any materials would exceed the 50 ft-lb screening criterion. The results of these evaluations are summarized in Reference [MA93] and were presented in the response to NRC Generic Letter 92-01 [MA92]. As a result of these evaluations, NMPC concluded that an Appendix X analysis must be performed for beltline plates G-8-1 and G-307-4. The results of the Appendix X analysis for Service Level A and B loadings were reported in Reference [MA93]. This report presents the results of the Service Level C and D loading analysis.

2.0 Material Model

The NMP-1 beltline plates were fabricated using A302B modified (A302M) steel. At present, sufficient J-R data are not available to construct an A302M model. As discussed in Reference [MA93], the NMP-1 plates are best modelled using an A302B J-R material model. The A302B material model is fully described in Reference [MA93]. For Service Level C loadings, the J-R curve inputs are two sigma lower bound curves which are the same as for Service Levels A and B. However, for Service Level D analysis, Reference [ASME92] allows the use of J-R curves which are a best estimate representation for the vessel material being analyzed. Therefore, the best estimate, or mean, J-R curves, as a function of USE level, were determined. The J_{IC} versus USE model reported in Reference [MA93] was used to calculate the mean J_{IC} data given in Table 2-1. The 6T J_D-Δa data reported in Reference [HI89] were used to determine the J-R curves at the USE levels shown in Table 2-1. The 6T J_D-Δa data were reduced or increased by the difference between the 6T test J_{IC} value (525 in-lb/in^2) and the J_{IC} data listed in Table 2-1. The yield stress, modulus, and Poisson ratio used in the analysis are identical to the Reference [MA93] data.

Table 2-1

Mean J_{IC} Data as a Function of USE Level

USE (FT-LBS)	J_{IC} (IN-LB/IN^2)
10	79.2
20	158.3
30	237.5
40	316.6
50	395.8
60	474.9
70	554.1
80	633.2
90	712.4
100	791.5

3.0 Transient Selection

The ASME draft Appendix X does not specify procedures for calculating Level C and D service loadings since the combinations of loadings and material properties encountered in practice are too diverse. Therefore, the most limiting transients for Levels C and D, from a ductile fracture perspective, were identified as follows:

- The NMP-1 and NMP-2 plant documentation was carefully examined to identify potential limiting transients.
- A screening calculation was then performed to reduce the spectrum of transients to a few most likely candidates.
- Finite element calculations were performed on the reduced set of transients to determine the most limiting Level C transient and the most limiting Level D transient and the resultant loading.

3.1 Level C Transient Selection

The NMP-1 and NMP-2 updated FSARs and thermal cycle diagrams were reviewed to determine a spectrum of candidate Level C transients for further analysis. Prior to performing the screening calculations, it was not clear whether the rapid pressure loss transients or the slow depressurization transients would provide the largest combined pressure and thermal gradient loads. Therefore, the transients shown in Figure 3-1 were chosen for analysis since they bound all Level C transients in terms of cooldown rate. Table 3-1 lists the temperature/pressure variation at various times during the transient. The classification of the automatic blowdown transient and emergency cooldown transient as Level C events is consistent with the definition of the emergency condition transients. Figure 3-1 includes two events described in the Unit 1 updated FSAR (References [FSAR] and [CENC]) and the Unit 2 (References [STRS] and [TCD]) emergency condition automatic blowdown.

3.2 Level D Transient Selection

As with the Level C transient selection, the Level D transients were selected after careful examination of the NMP-1 and NMP-2 plant documentation. A set of transients were chosen which bound all Level D events in terms of cooldown rate. Plots of the selected transients are shown in Figures 3-2 through 3-5 (pressure/temperature profile data are also given in Tables 3-2 and 3-3.) The NMP-2 faulted condition events are specified based on the Reference [NEDC] analysis. The events included for consideration include the break spectrum for the recirculation line breaks, the steam line break, core spray line break, and the feedwater line break.

3.3 Screening Analysis

3.3.1 Model Description

The transients described earlier were analyzed using a simple linear elastic fracture mechanics model to determine those transients which require a detailed finite element analysis to determine the limiting loads. The temperature difference across the vessel wall for the Level C transients was calculated using the TRUMP/MPM code [TRUMP]. The NMP-1 vessel was modelled using cylindrical coordinates. The vessel is 7.281 in. thick with an inner radius of 106.5 inches. The 0.1563 in. stainless steel liner was modelled as having the physical properties of 316 SS, and the rest of the vessel thickness was modelled as A302B ferritic steel. A total of 17 radial nodes, each of approximately 0.44 in. thickness, were used to discretize the vessel thickness. A nodel temperature boundary condition was applied at the ID surface of the vessel. The surface node was modelled as being in thermal equilibrium with the downcomer fluid temperature. This assumption leads to conservative through wall gradient estimates, particularly for the Level D transients during which phase change occurs. Therefore, the initial temperature of all vessel nodes were set to 500°F.

Once the temperature difference across the wall was calculated, the relative contribution of the pressure loading and the thermal loading was approximated using the linear elastic fracture mechanics model given in Appendix G to the ASME code. It should be emphasized that these equations are based on linear elastic fracture mechanics principles and are strictly applicable for thermal ramps of up to 100°F/hr. Nevertheless, for screening purposes, these equations are adequate for assessing the relative contributions of the pressure and thermal loads to the total crack tip stress intensity for the various Level C and D events. Appendix G uses the following equations to calculate the stress intensities:

$$K = K_{IM} + K_{IT} \tag{3-1}$$

where,

$K_{IM} = M_M \sigma$ = membrane stress intensity factor (ksi $\sqrt{\text{in}}$)

$K_{IT} = M_T \Delta T$ = stress intensity factor due to thermal gradient (ksi $\sqrt{\text{in}}$)

M_M = ASME membrane factor ($\sqrt{\text{in}}$)

M_T = ASME thermal factor (ksi $\sqrt{\text{in}}$/°F)

ΔT = temperature difference across vessel wall (°F)

σ = stress (ksi)

$$\sigma = \frac{(A^2 + B^2)}{(B^2 - A^2)} P \qquad (3-2)$$

A = vessel inner radius (in.)

B = vessel outer radius (in.)

P = internal pressure (psig)

Since the Appendix X flaw growth criterion is more severe at deep crack depths under Level C and D event loads, the screening calculations were performed assuming a one-quarter thickness flaw. This flaw exceeds the deepest postulated flaw analyzed under the Level C and D analysis.

3.3.2 Level C Transient Analysis

The blowdown transients are terminated when the pressure reaches 35 psig to account for the containment pressure level at that time in the transient. In the TRUMP/MPM calculations, these transients were extended to longer times, conservatively assuming a 300°F/hr cooldown to a 212°F vessel ID temperature. The thermal gradient and pressure data for the Level C transients are summarized in Table 3-4. Based on the data in Table 3-4, the 250°F/7.5 min. Blowdown and the Thermal Transient Blowdown are limiting in terms of ductile fracture. Therefore, detailed finite element calculations were performed for both of these transients to determine the most limiting vessel wall stress distribution.

3.3.3 Level D Transient Analysis

Since the Level D transient depressurization occurs over a relatively short time period, and it has been assumed that the downcomer fluid temperature equals the wall surface temperature for the purpose of performing a screening analysis, it was not necessary to perform a thermal transient heat transfer analysis for the Level D transients. Based on the Level C analysis results, the vessel wall ΔT is approximately equal to 528°F minus the current downcomer fluid temperature for the initial five minutes of the transient. Therefore, the crack tip stress intensities can be calculated directly. It should be recognized that these assumptions are increasingly over-conservative after the initial five minutes of the transient.

The results of the stress intensity factor calculations for the Service Level D

transients are shown in Tables 3-5 and 3-6. Based on these calculations, the Steam Line Break Transient, NMP-2 Recirculation Line Break Transient, and the NMP-1 Recirculation Line Break Transient were analyzed in further detail using the finite element method. The other transients yield lower peak stress intensities. In addition, the stress intensity factor estimates for the other transients are very conservative since a significant portion of the transient is spent in a steam forced convection and/or subcooled free convection heat transfer regime.

3.3.4 Summary of Candidate Transients

A simplified model was developed to determine the limiting Service Level C and D transients. Perfect heat transfer between the downcomer fluid and the vessel wall surface was assumed to provide conservative estimates of the through wall thermal gradient. A quarter thickness flaw was assumed and the ASME Appendix G linear elastic model was used to estimate the crack tip stress intensities. Based on the simplified model for screening calculations, the most limiting transients, from a ductile fracture perspective, are summarized in Tables 3-7 and 3-8.

Table 3-1
Level C Transient Temperature/Pressure Variation as a
Function of Time Measured From the Initiation of the Event

Emergency Condition
Level C Transients

Unit 1 Design Basis 250°F/7.5 min Blowdown			*Unit 2 Design Basis Thermal Transient Blowdown*			*Unit 1 Emergency Cooldown 300°F/hr*			*Unit 1 SB-LOCA ADS Blowdown*		
Time (minutes)	Pressure (PSIA)	Temp (°F)	Time (minutes)	Pressure (PSIA)	Temp (°F)	Time (minutes)	Pressure (PSIA)	Temp (°F)	Time (minutes)	Pressure (PSIA)	Temp (°F)
0	1045	528*	0	1045	528*	0	1045	528*	0	1045	528*
2	515	470	3.3	184	375	10	556	478	1	730	508
4	196	380	10	121	342	20	344	430	7.7	110	335
6	87	318	15	87	318	30	191	378	-	-	-
7.5	48	278	20	62	295	40	103	330	-	-	-
-	-	-	25	50	281	50	50	281	-	-	-
-	-	-	-	-	-	60	20	228	-	-	-

*Nominal Subcooling 100% Power Rated Feedwater Temperature

Table 3-2
Level D Steam Line Break Temperature/Pressure Variation as a Function of Time Measured From the Initiation of the Event

Steam Line Break

Reference (1)			Oyster Creek Analysis Reference (2)		
Time (sec)	Pressure (PSIA)	Temp °F	Time (sec)	Pressure (PSIA)	Temp °F
0	1045	528*	0	1050	552
20	660	497	70	120	350
40	310	420	300	0	212
60	200	381	450	35	281
80	130	347			
100	90	320			
120	60	292			
140	40	267			
160	31	252			
180	25	240			
300	15	212			

Reference 1 - NMP1 SAFER/CORECOOL/GESTR-LOCA Analysis
NEDC-31456P, 1987, NMP1, Figure A017

Reference 2 - Oyster Creek Report GENE-523-70-0692 August '92 "Oyster Creek Vessel Fracture Mechanics Analysis" for upper shelf energy requirement. Figure 5-6 Page 5-13

*Nominal Subcooling 100% Power Rated Feedwater Temperature

Table 3-3
Level D Recirculation Line Break Spectrum Temperature/Pressure Variation as a Function of Time Measured From Initiation of the Event

Recirculation Line Break Spectrum

DBA			40 % DBA			1 ft^2			.5 ft^2			.1 ft^2			.05 ft^2		
Time (sec)	Press PSIA	Temp (°F)	Time (sec)	Press PSIA	Temp (°F)	Time (sec)	Press PSIA	Temp (°F)	Time (sec)	Press PSIA	Temp (°F)	Time (sec)	Press PSIA	Temp (°F)	Time (sec)	Press PSIA	Temp (°F)
0	1045	-	0	1045	528	0	1045	-	0	1045	-	0	1045	-	0	1045	-
10	760	512	20	860	527	20	920	535	50	900	539	100	960	540	240	900	532
20	300	417	30	660	497	50	800	518	100	800	518	180	860	527	280	800	518
30	80	312	40	430	452	70	600	486	150	520	471	200	790	517	300	730	508
40	40	267	50	260	404	90	400	445	180	280	411	300	480	463	360	560	479
50	20	228	60	150	358	100	320	423	200	200	381	340	400	445	440	400	445
80	15	212	70	100	328	130	170	368	300	80	312	400	300	417	500	320	423
-	-	-	90	60	293	150	120	341	400	40	267	470	220	390	600	210	385
-	-	-	320	15	212	200	70	303	-	-	-	-	-	-	700	110	335
-	-	-	-	-	-	300	40	267	-	-	-	-	-	-	800 *	80	312
-	-	-	-	-	-	-	-	-	-	-	-	-	-	-	1080 *	40	267

Table 3-4
Stress Intensity Factor Estimates for Service Level C Transients[1]

	250°F/7.5 Min. Blowdown					Thermal Transient Blowdown					Emergency Cooldown 300°F/hr.				
Time (Min.)	P	ΔT	K_{IM}	K_{IT}	K	P	ΔT	K_{IM}	K_{IT}	K	P	ΔT	K_{IM}	K_{IT}	K
2	1030	57	40	18	58	1030	91	40	29	68	1030	10	40	3	43
3	500	101	19	32	51	500	137	19	43	62	1030	15	40	5	45
4	500	146	19	46	65	169	155	7	49	55	1030	20	40	6	46
6	181	206	7	65	72	169	162	7	51	57	1030	30	40	9	49
8	33	244	1	77	78	169	167	7	53	59	1030	39	40	12	52
10	33	245[2]	1	77	78	169	168[2]	7	53	59	541	48	21	15	36
20											329	81	13	25	38
30											176	107	7	34	40
40											88	120	3	38	41
50											35	130	1	41	42
60											5	140[2]	0	44	44

[1] Units - P=psig; ΔT=max temp diff. (°F); K_{IM}=membrane stress intensity (ksi $\sqrt{in}$); K_{IT}=thermal stress intensity (ksi $\sqrt{in}$); K=total stress intensity (ksi $\sqrt{in}$)

[2] Peak wall thermal gradient

Table 3-5A
Stress Intensity Factor Estimates for Service Level D Transients[1]

	Steam Line Break					Feedwater Line Break					Core Spray Line Break					Recirc. Line Break NMP-2					Recirc. Line Break DBA					Recirc. Line Break 40% DBA				
Time (Sec.)	P	ΔT	K_{IM}	K_{IT}	K	P	ΔT	K_{IM}	K_{IT}	K	P	ΔT	K_{IM}	K_{IT}	K	P	ΔT	K_{IM}	K_{IT}	K	P	ΔT	K_{IM}	K_{IT}	K	P	ΔT	K_{IM}	K_{IT}	K
10						945	0	36	0	36											745	16	29	5	34					
15																20	259	1	82	83										
20	645	31	25	10	35																285	111	11	35	46	845	1	33	0	33
30																					65	216	3	68	71	645	31	25	10	35
40	295	108	11	34	45																25	261	1	82	83	415	76	16	24	40
50																					5	300	0	94	94	245	124	9	39	48
60	185	147	7	46	53																					135	170	5	53	58
70																										85	200	3	63	66
75						785	10	30	3	33																				
80	115	181	4	57	61																0	316	0	99	99					
90																										45	235	2	74	76
100	75	208	3	65	68	705	22	27	7	34																				
120	45	236	2	74	76																									
130																														
140	25	261	1	82	83																									
145											785	10	30	3	33															
150																														

[1] Units- P=psig; ΔT=max temp diff. (°F); K_{IM}=membrane stress intensity (ksi √in); K_{IT}=thermal stress intensity (ksi √in); K=total stress intensity (ksi √in)

Table 3-5B
Stress Intensity Factor Estimates for Service Level D Transients[1]

	Steam Line Break					Feedwater Line Break					Core Spray Line Break					Recirc. Line Break NMP-2					Recirc. Line Break DBA					Recirc. Line Break 40% DBA				
Time (Sec.)	P	ΔT	K_M	K_T	K	P	ΔT	K_M	K_T	K	P	ΔT	K_M	K_T	K	P	ΔT	K_M	K_T	K	P	ΔT	K_M	K_T	K	P	ΔT	K_M	K_T	K
160	16	276	1	87	88																									
175											715	28	28	7	35															
180	10	288	0	91	91																									
200						385	84	15	26	41																				
285											385	84	15	26	41															
300	0	316	0	99	99	125	175	5	55	60						35	306	1	97	98										
320																										0	316	0	99	99
360																														
400						65	< 216	3	<68	<71	205	138	8	43	51															
440																														
470																														
500						35	< 247	1	<78	<79	115	181	4	57	61															
600																														
630											35	< 247	1	<78	<79															
700						0	< 316	0	<99	<99																				
750											0	< 316	0	<99	<99															
1080																														

[1] Units- P=psig; ΔT=max temp diff. (°F); K_M=membrane stress intensity (ksi √in); K_T=thermal stress intensity (ksi √in); K=total stress intensity (ksi √in)

Table 3-6A
Stress Intensity Factor Estimates for Service Level D Transients[1]

	Recirc. Line Break 1 ft²					Recirc. Line Break 0.5 ft²					Recirc. Line Break 0.1 ft²					Recirc. Line Break 0.05 ft²				
Time Sec.	P	ΔT	K_{IM}	K_{IT}	K	P	ΔT	K_{IM}	K_{IT}	K	P	ΔT	K_{IM}	K_{IT}	K	P	ΔT	K_{IM}	K_{IT}	K
10																				
15																				
20	905	7	35	2	37															
30																				
40																				
50	785	10	30	3	33	885	11	34	3	37										
60																				
70	585	42	23	13	36															
75																				
80																				
90	385	83	15	26	41															
100	305	105	12	33	45	785	10	30	3	33	945	12	36	4	40					
120																				
130	155	160	6	50	56															
140																				
145																				
150	105	187	4	59	63	505	57	19	18	37										

[1] Units- P=psig; ΔT=max temp diff. (°F); K_{IM}=membrane stress intensity (ksi √in); K_{IT}=thermal stress intensity (ksi √in); K=total stress intensity (ksi √in)

Table 3-6B
Stress Intensity Factor Estimates for Service Level D Transients[1]

	Recirc. Line Break 1 ft²					Recirc. Line Break 0.5 ft²					Recirc. Line Break 0.1 ft²					Recirc. Line Break 0.05 ft²				
Time Sec.	P	ΔT	K_{IM}	K_{IT}	K	P	ΔT	K_{IM}	K_{IT}	K	P	ΔT	K_{IM}	K_{IT}	K	P	ΔT	K_{IM}	K_{IT}	K
160																				
175																				
180						265	117	10	37	47	845	1	33	0	33					
200	55	225	2	71	73	185	147	7.	46	53	775	11	30	3	33					
280																785	10	30	3	33
300	25	261	1	82	83	65	216	3	68	71	465	65	18	20	38	715	20	28	6	34
320																				
360																				
400						25	261	1	82	83	385	111	15	35	50					
440	0	<316	0	<99	<99											385	83	15	26	41
470											205	138	8	43	51					
500						0	<316	0	<99	<99						305	105	12	33	45
600																195	143	8	45	53
630																				
700																95	193	4	61	65
800																65	<216	3	<68	<71
930											0	<316	0	<99	<99					
1080																25	<216	1	<82	<83
1420																0	<316	0	<99	<99

[1] Units- P=psig; ΔT=max temp diff. (°F); K_{IM}=membrane stress intensity (ksi √in); K_{IT}=thermal stress intensity (ksi √in); K=total stress intensity (ksi √in)

Table 3-7

Level C Transients for Finite Element Analysis

NMP-1 Design Basis 250°F/7.5 Min. Blowdown[1]				NMP-2 Design Basis Thermal Transient Blowdown[2]			
Time (Min.)	Pressure (psig)	Temp. (°F)	Heat Transfer Coefficient h=BTU/(hr ft²F)	Time (Min.)	Pressure (psig)	Temp. (°F)	Heat Transfer Coefficient h=BTU/(hr ft²F)
0	1030	528	10,000	0	1030	528	10,000
2	500	470	10,000	3.3	169	375	10,000
4	181	380	10,000	10	106	342	10,000
6	72	318	10,000	15	72	318	10,000
7.5	33	278	10,000	20	47	295	10,000
20.7	0	212	500	25	35	281	10,000
				38.8	0	212	500

[1] NMP-1 Updated FSAR

[2] Reference [STRS]

Table 3-8
Level D Transients for Finite Element Analysis

Steam Line Break [1]				Recirculation Line Break[2] - NMP-2				Recirculation Line Break[1] - NMP-1 DBA			
Time (Sec.)	Pressure (psig)	Temp (°F)	Heat Transfer Coefficient h=BTU/(hr ft²F)	Time (Sec.)	Pressure (psig)	Temp. (°F)	Heat Transfer Coefficient h=BTU/(hr ft²F)	Time (Sec.)	Pressure (psig)	Temp (°F)	Heat Transfer Coefficient h=BTU/(hr ft²F)
0	1030	528	10,000	0	1030	528	69,188	0	1030	528	10,000
20	645	497	10,000	15	35	281	164	10	745	512	10,000
40	295	420	10,000	20	23	264	164	15	474	464	164
60	185	381	10,000	60	23	264	164	20	285	417	164
80	115	347	10,000	100	18	256	164	30	65	312	164
100	75	320	10,000	200	8	235	164	40	25	267	164
120	45	292	10,000	300	3.5	222	164	50	5	228	164
140	25	267	10,000	1300	0	212	500	80	0	212	500
160	16	252	10,000								
180	10	240	10,000								
300	0	212	10,000								
380	0	212	164								
400	0	212	500								

1 Reference [NEDC]
2 References [NMP2TC], [STRS], and [NMP1DP]

Emergency Condition
Level C Transients

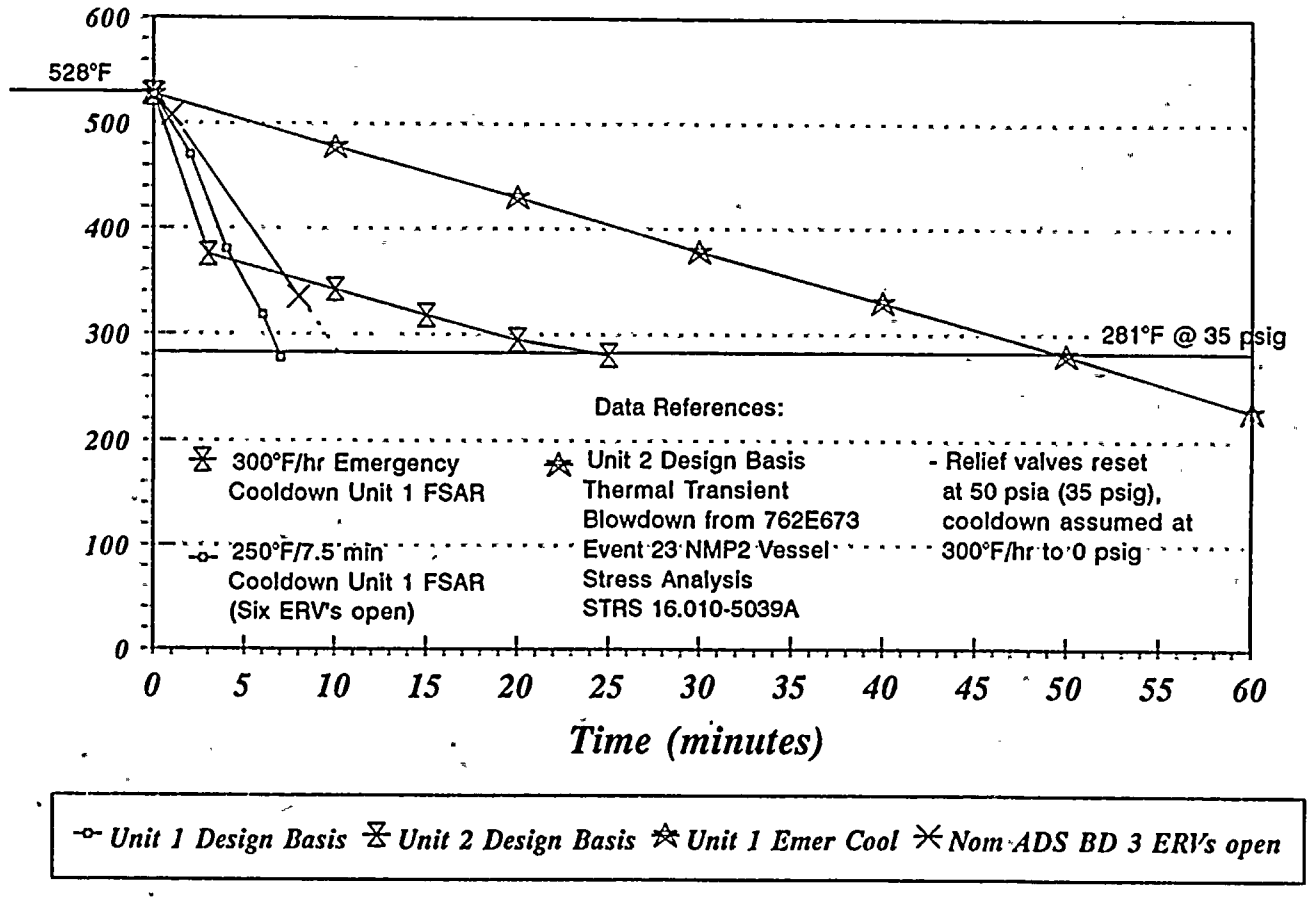

Figure 3-1
Level C Transients Analyzed to Determine the
Most Limiting Transient for NMP-1

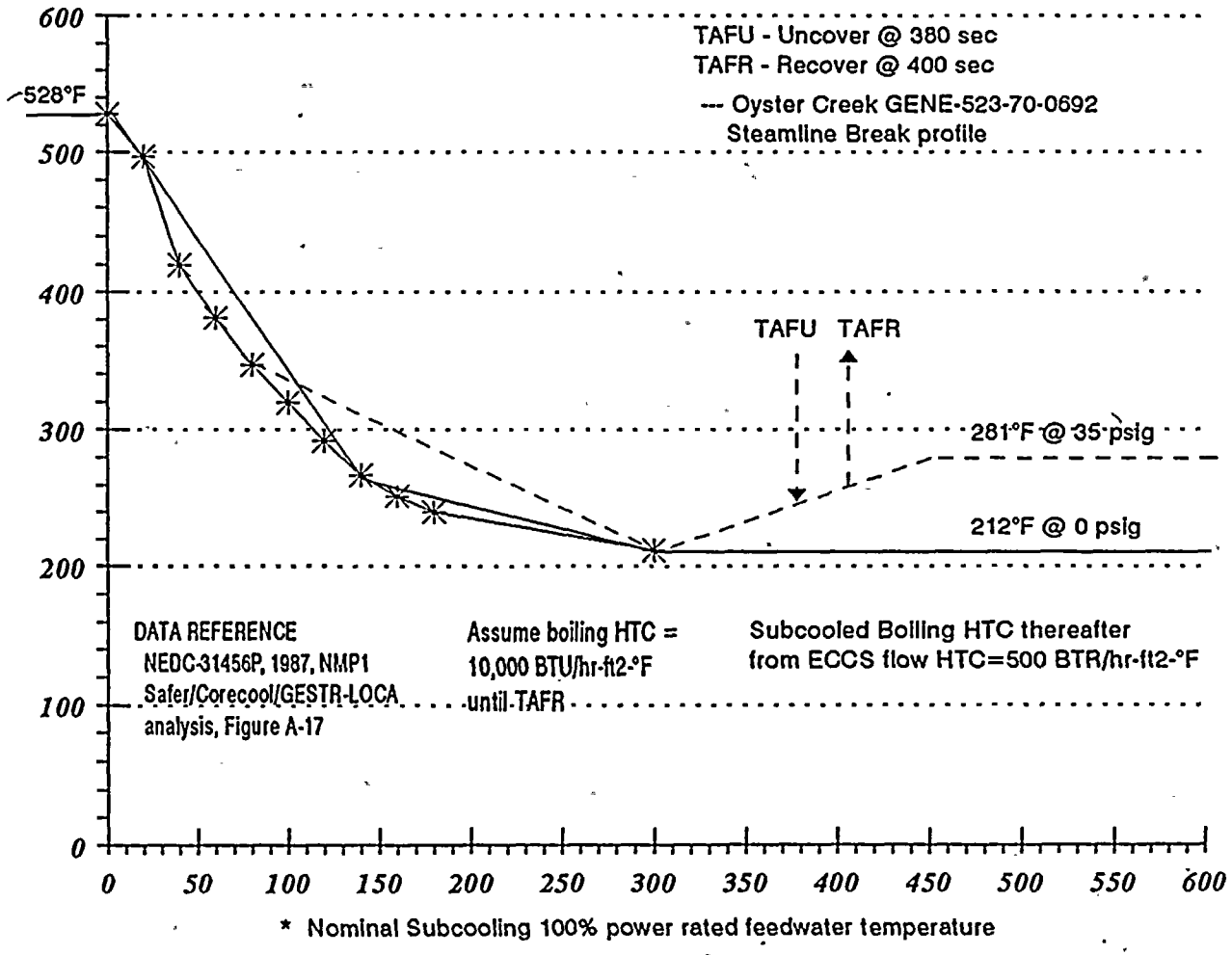

Figure 3-2
Level D Steam Line Break Transient Pressure Profile

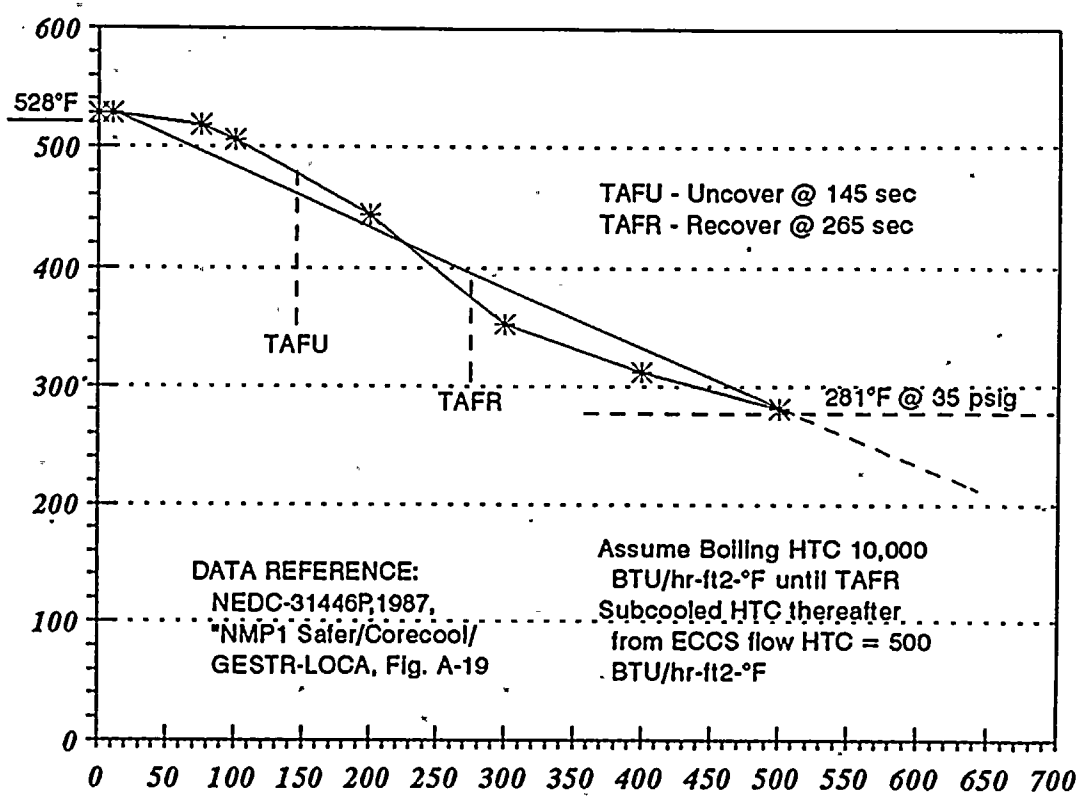

Time (sec)	0	10	75	100	200	300	400	500
Pressure (PSIA)	1,045	960	800	720	400	140	80	50
Saturated Temp (°F) *	528*	528*	518	506	444	353	312	281

* Nominal Subcooling 100% power rated feedwater temperature

Figure 3-3
Level D Feedwater Line Break Transient Pressure Profile

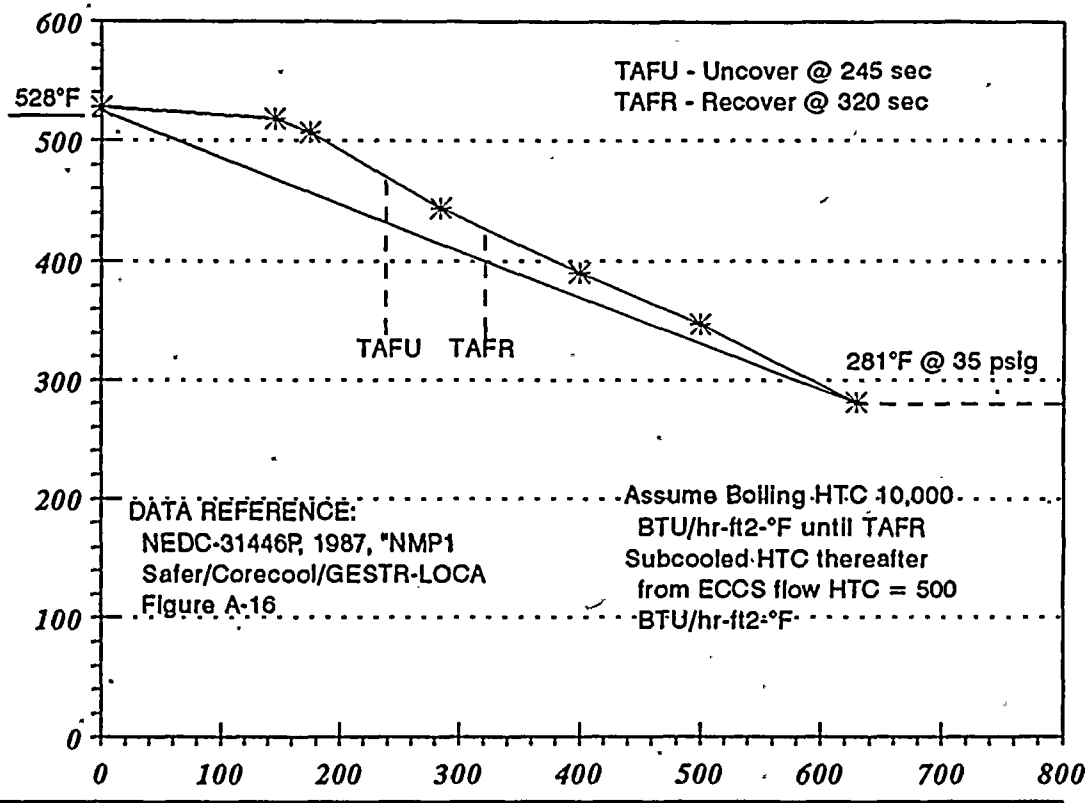

Time (sec)	0	145	175	285	400	500	630
Pressure (PSIA)	1,045	800	730	400	220	130	50
Saturated Temp (°F) *	528 *	518	507	444	390	347	281

* Nominal Subcooling 100% power rated feedwater temperature

Figure 3-4
Level D Core Spray Line Break Pressure Profile

Recirculation Line Break Spectrum

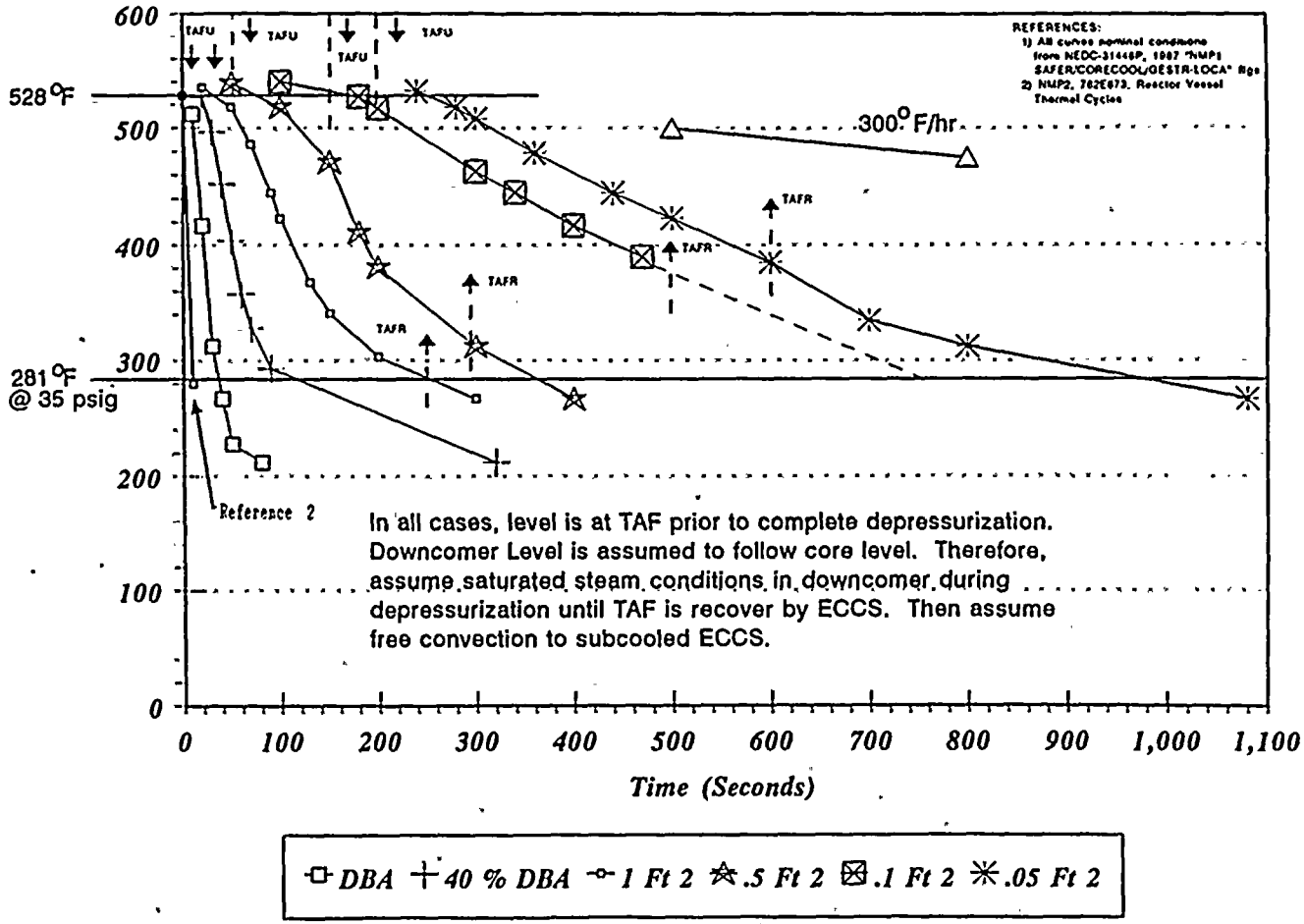

Figure 3-5
Level D Recirculation Line Break Spectrum Pressure Profile

4.0 Finite Element Analysis

The candidate transients listed in Tables 3-7 and 3-8 were analyzed using the finite element method to determine the most severe Level C and Level D loadings. The WELD3 finite element code package [WELD3] was used to perform the calculations.

4.1 Model Description

The WELD3 model assumes axisymmetric behavior. A single column of elements was used, thus making the solution essentially one dimensional (i.e., temperatures and stresses only depend on the radial position within the vessel wall). The finite element grid is shown in Figure 4-1. Elements 1 and 2 represent the cladding. The cladding inner surface radius is 106.344 inches, the base metal/clad interface is at 106.5 inches, and the vessel outer radius is 113.781 inches. The axial dimension of the model is 0.15 inches.

For thermal modeling, the outer vessel surface was treated as perfectly insulated. The inner surface has a prescribed heat transfer coefficient and fluid temperature (both functions of time). All heat flow is radial. Temperature dependent properties were used in the thermal analysis.

The mechanical model is constrained to have a uniform axial strain so that plane sections remain plane. The average axial stress and the internal pressure are input to the model based on the pressure transient input. Thermal transients are input via element temperatures. Temperature dependent properties are also used for the stress calculations.

The WELD3 calculations assumed linear elastic behavior for both the cladding and base metal so as to be consistent with the use of the small scale yielding assumption (linear elastic fracture mechanics with plastic zone corrections) in the subsequent fracture mechanics analyses.

4.2 Finite Element Analysis Results

Two Level C cases and three Level D cases were analyzed. The transient thermal and pressure boundary conditions are described in Tables 3-7 and 3-8. Although the pressure and thermal loadings could be analyzed separately due to the use of linear elasticity, it was judged more expedient to combine the loadings.

The cladding has a different coefficient of thermal expansion than the base metal. This impacted the analysis in several ways. First, there will be some residual stress even when the vessel is at a uniform temperature. Assuming that the vessel is 100% stress free at the stress relief temperature of 1150°F, the original cooling to 528°F induced tensile residual stresses in the cladding thus contributing to crack tip stress intensity factors. This uniform cooling was modeled in a separate analysis to determine the level of initial residual stress. The difference in thermal expansion behavior also results in discontinuous

axial and hoop stresses across the material interface. Since the fracture mechanics evaluation involves fitting the stresses with a cubic polynomial, this discontinuous behavior impacts the quality of the polynomial fits. Therefore, as described in Section 5.0, the fracture mechanics model was configured to minimize the sensitivity of the analysis to the effects of stress field discontinuities at the interface.

Figure 4-2 shows the axial and hoop residual stresses that exist due to uniform cooling from a stress free condition at 1150°F to 528°F. This residual stress was not included in the stress distribution plots for the various Level C and Level D transients that follow. This approach was adopted as part of the approach to more accurately handle the discontinuous stress field. The final stress distributions do include the differential expansion coefficient effects due to cooling from 528°F during the transient. The method for including the residual stress load in the fracture mechanics analysis is described in Section 5.0.

The WELD3 stress output for each analysis was scanned for the time of the most severe stresses induced by the combined transient thermal and pressure loading. Since crack depths of no larger than one inch are of interest [ASME92], the time at which the stresses would be most severe for a one inch deep crack was identified. This was done without actually calculating stress intensity factors for each transient stress distribution and was possible only because the stresses over the inner inch of the wall tended to peak at about the same point in time. Figures 4-3 through 4-10 contain plots of the transient temperatures and stresses. The times of the most damaging stresses for crack depths of about an inch are plotted with a solid line. Temperatures and stresses at other times are plotted using broken lines. It can be seen from these plots that for deeper cracks, the critical time would tend to be later in the transient. For very shallow cracks, slightly larger stress intensity factors may occur at earlier times than for the identified times. Table 4-1 summarizes the results of the WELD3 analyses.

4.3 Limiting Transients

The hoop and axial stress behaviors are very similar and tend to experience their peak values at about the same time. The magnitudes of the hoop stresses tend to be larger than the axial stresses. Without inputting these stresses into a fracture mechanics analysis it is not possible to determine which stress component is limiting. As discussed further in Section 5.0, the axially oriented flaw (hoop stress loading) is the limiting case.

Of the two Level C cases considered, the "NMP-1 Design Basis 250°F/7.5 min. Blowdown" resulted in the larger stresses. Of the three Level D cases, the "Steam Line Break" resulted in the largest stresses. As shown in Figures 4-3 through 4-5, the time dependence of the heat transfer coefficient plays an important role in defining the limiting Level D transient. In particular, although the Steam Line Break is not the most rapid depressurization transient, it is limiting since the heat transfer is more efficient over the first 300 seconds of the event.

Table 4-1

Summary of Peak Cladding and Peak Base Metal Stresses
at the Indicated Times (stress units are ksi)

Case	Critical Time	Clad		Base	
		Hoop	Axial	Hoop	Axial
residual	NA	20.6	20.0	-0.7	-1.3
C1	9.15 min	60.6	50.2	40.5	29.8
C2	6.65 min	42.6	34.8	29.6	21.5
D1	240 sec	78.4	65.9	52.3	39.4
D2	500 sec	47.7	39.5	31.7	23.2
D3	320 sec	65.5	54.6	43.9	32.7

C1: NMP-1 Design Basis 250°F/7.5 min. Blowdown
C2: NMP-2 Design Basis Thermal Transient Blowdown
D1: Steam line Break
D2: Recirculation Line Break NMP-2
D3: Recirculation Line Break NMP-1 DBA

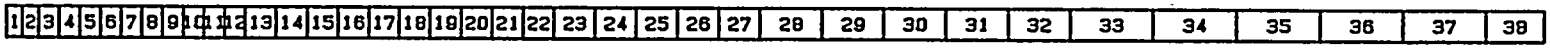

Figure 4-1
One Dimensional Finite Element Mesh for NMP-1 Pressure Vessel Analysis

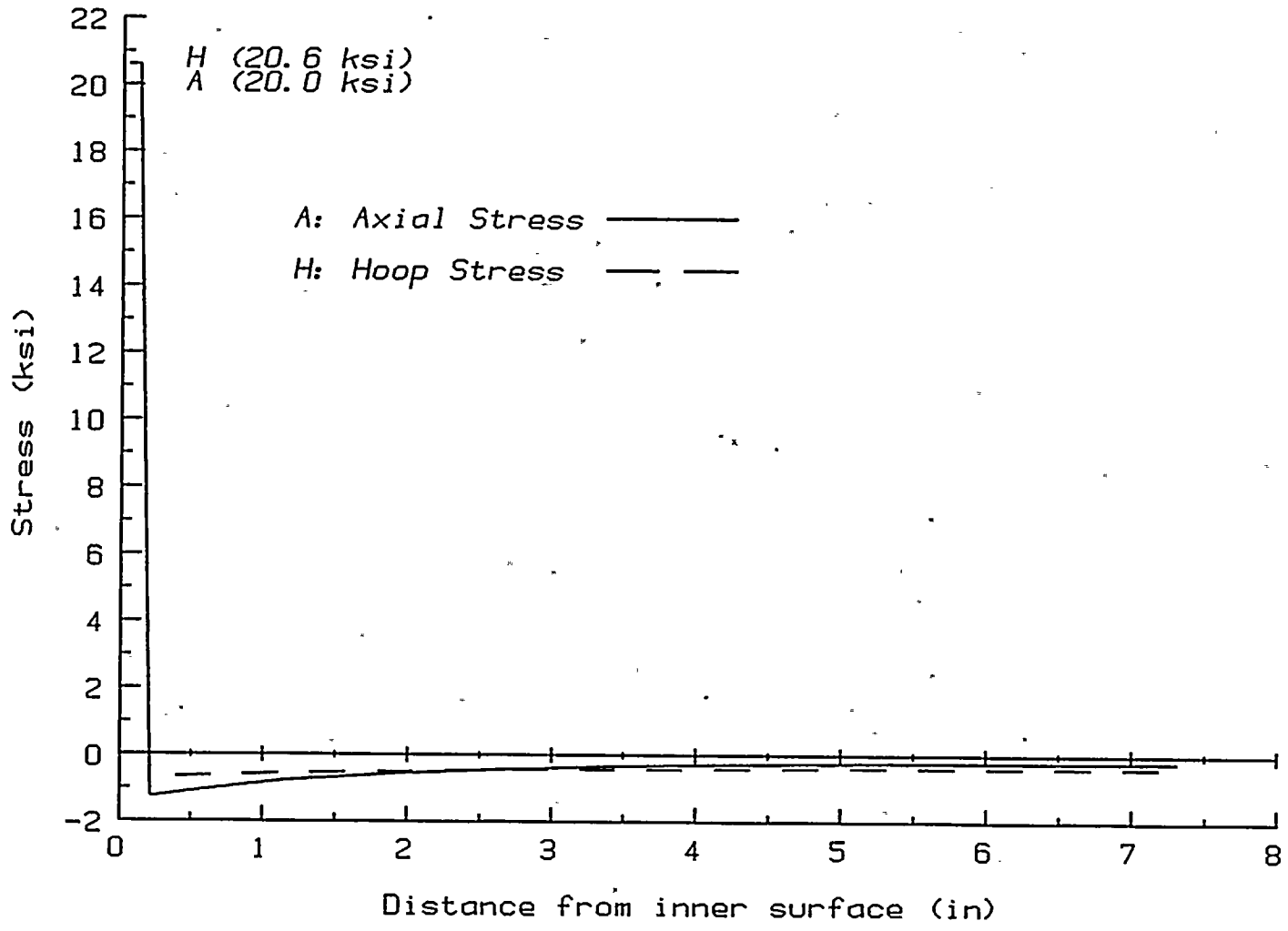

Figure 4-2
Residual Stress at 528°F Due to Cladding Differential Expansion

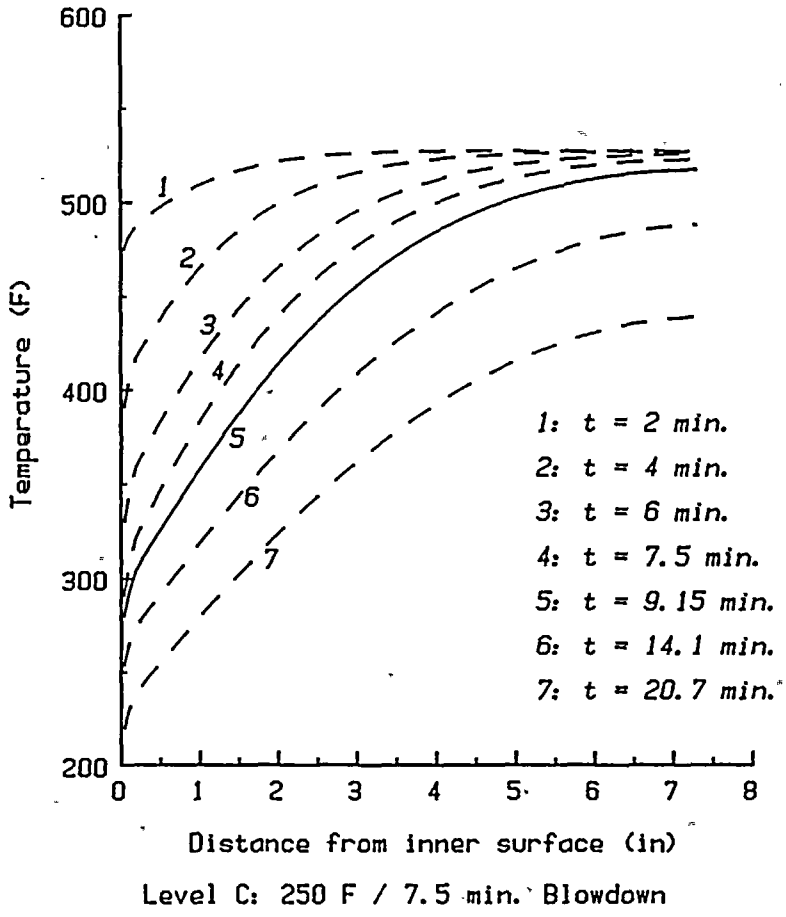

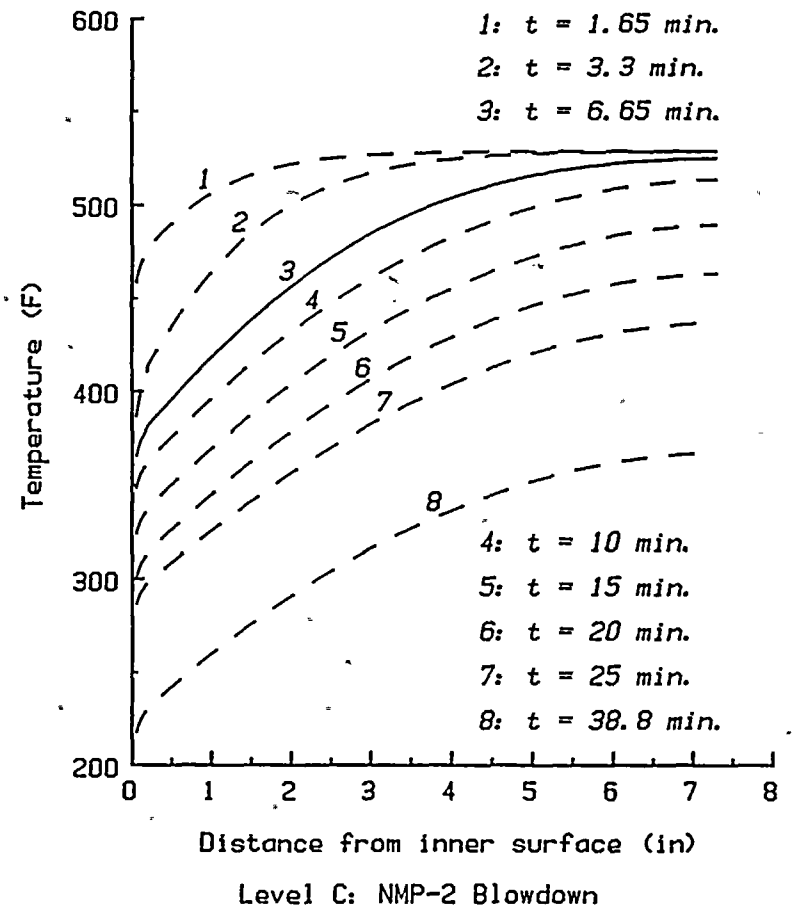

Figure 4-3
Pressure Vessel Thermal Gradients for Level C Transients

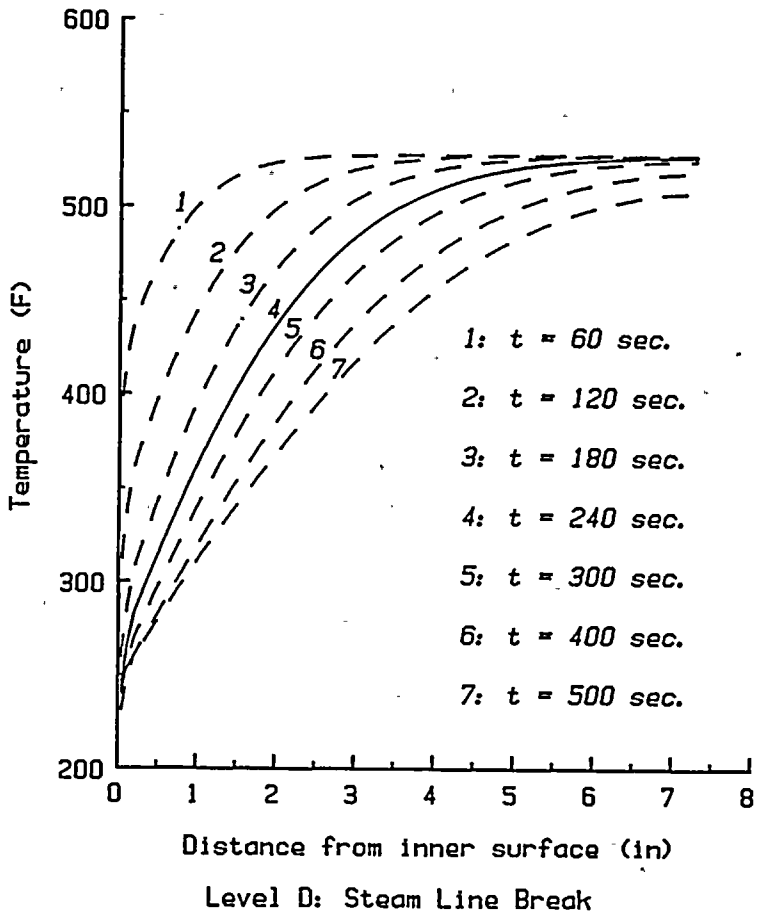

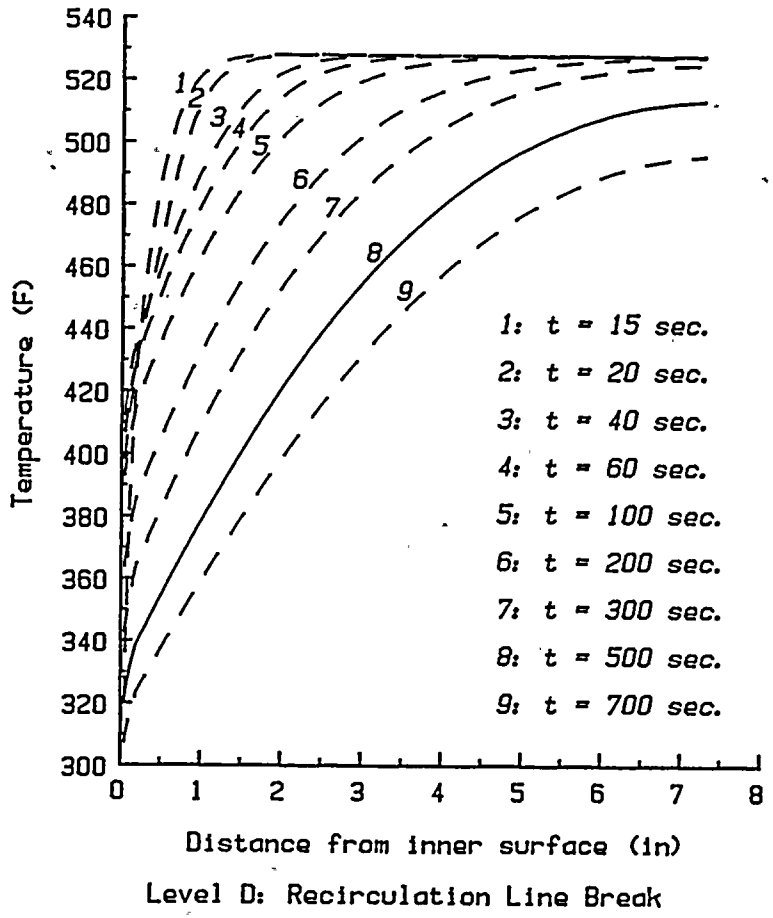

Figure 4-4
Pressure Vessel Thermal Gradients for Level D Transients

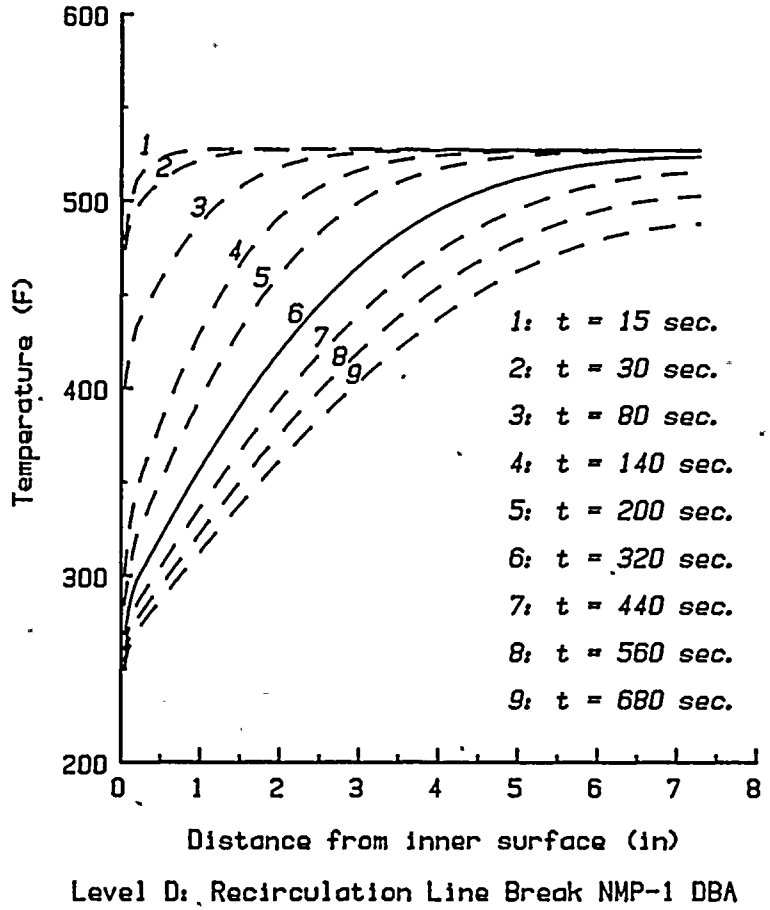

Figure 4-5
Pressure Vessel Thermal Gradients for Level D Transients

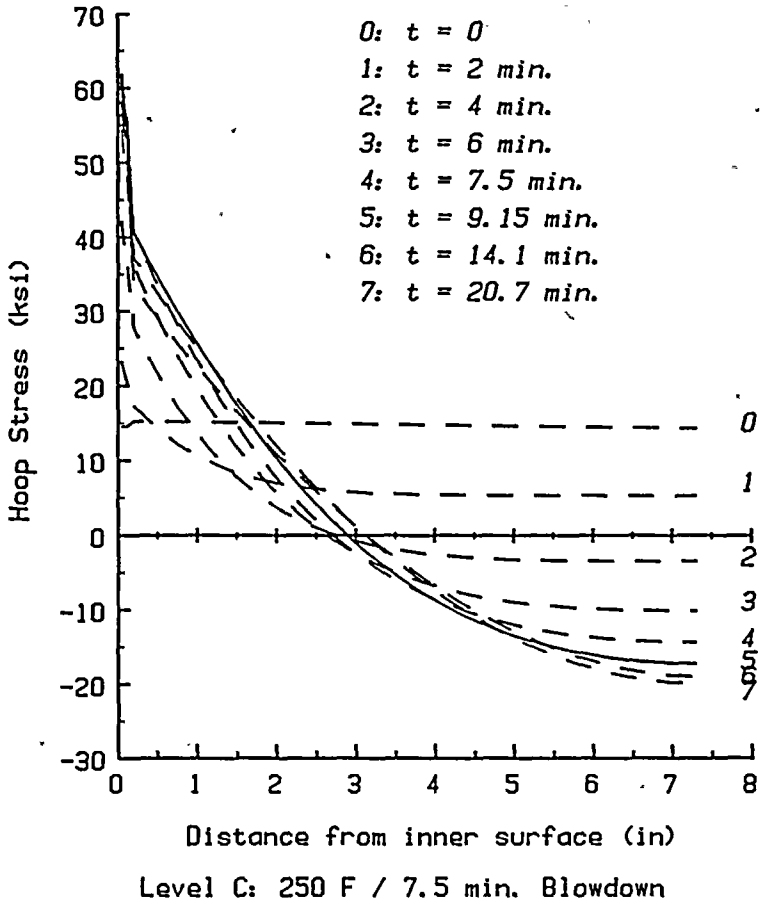

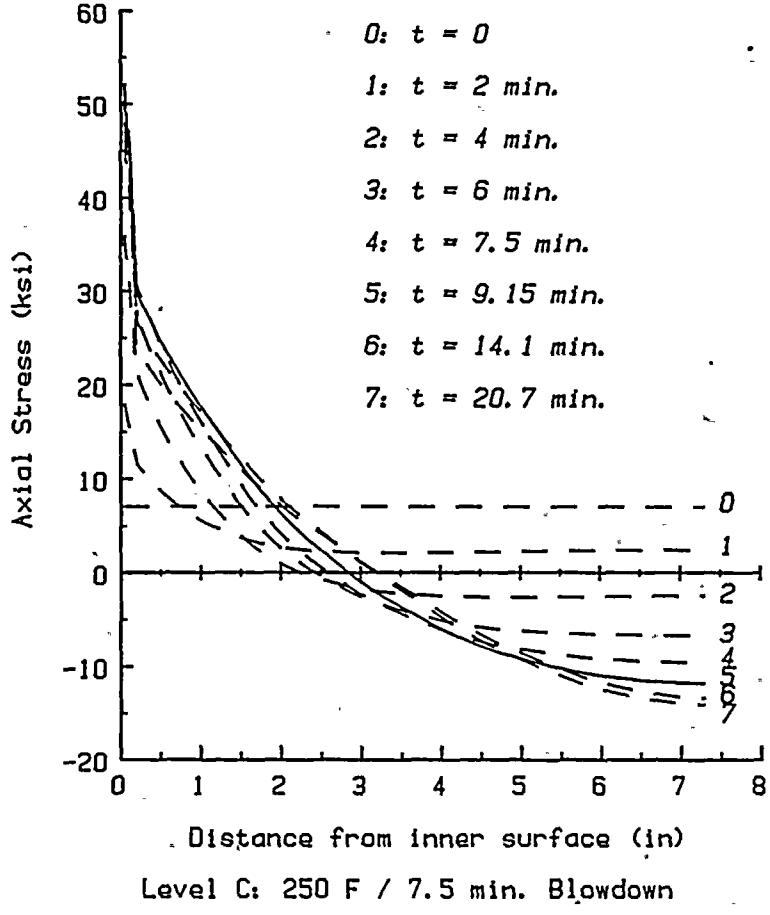

Figure 4-6
Axial and Circumferential Stress Distributions for Level C 250°F/7.5 Min. Blowdown

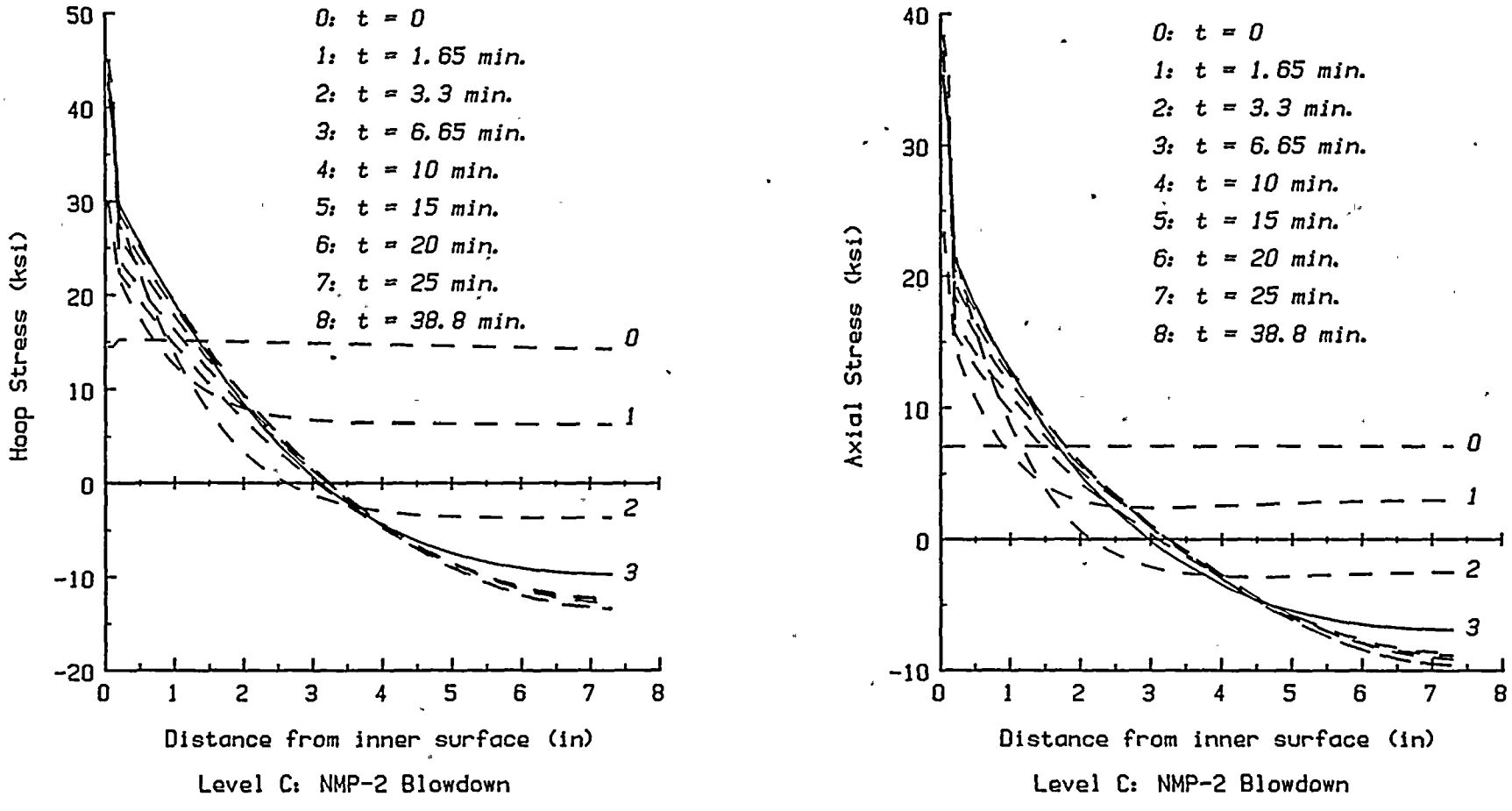

Figure 4-7
Axial and Circumferential Stress Distributions for Level C NMP-2 Blowdown

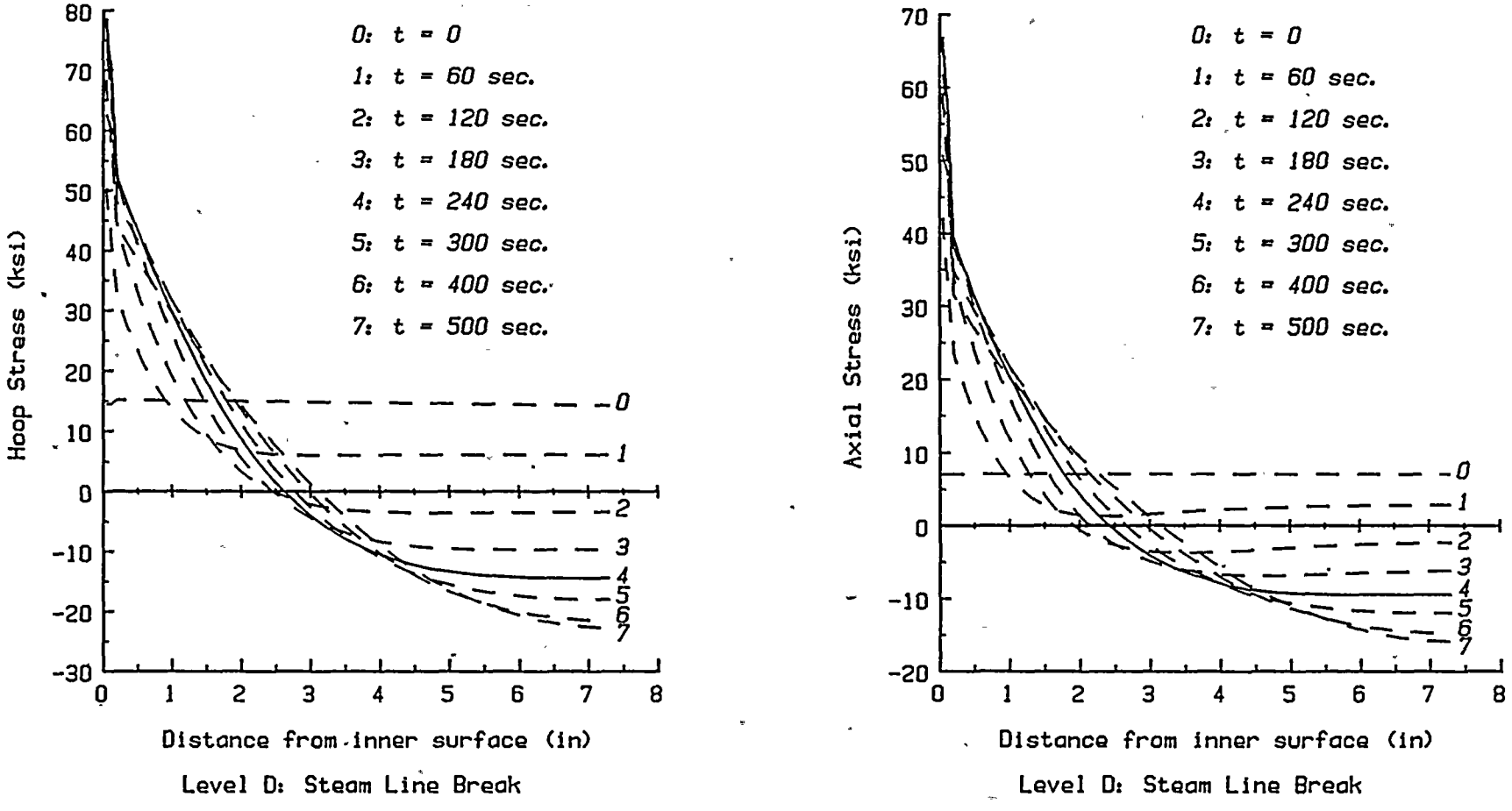

Figure 4-8
Axial and Circumferential Stress Distributions for Level D Steam Line Break

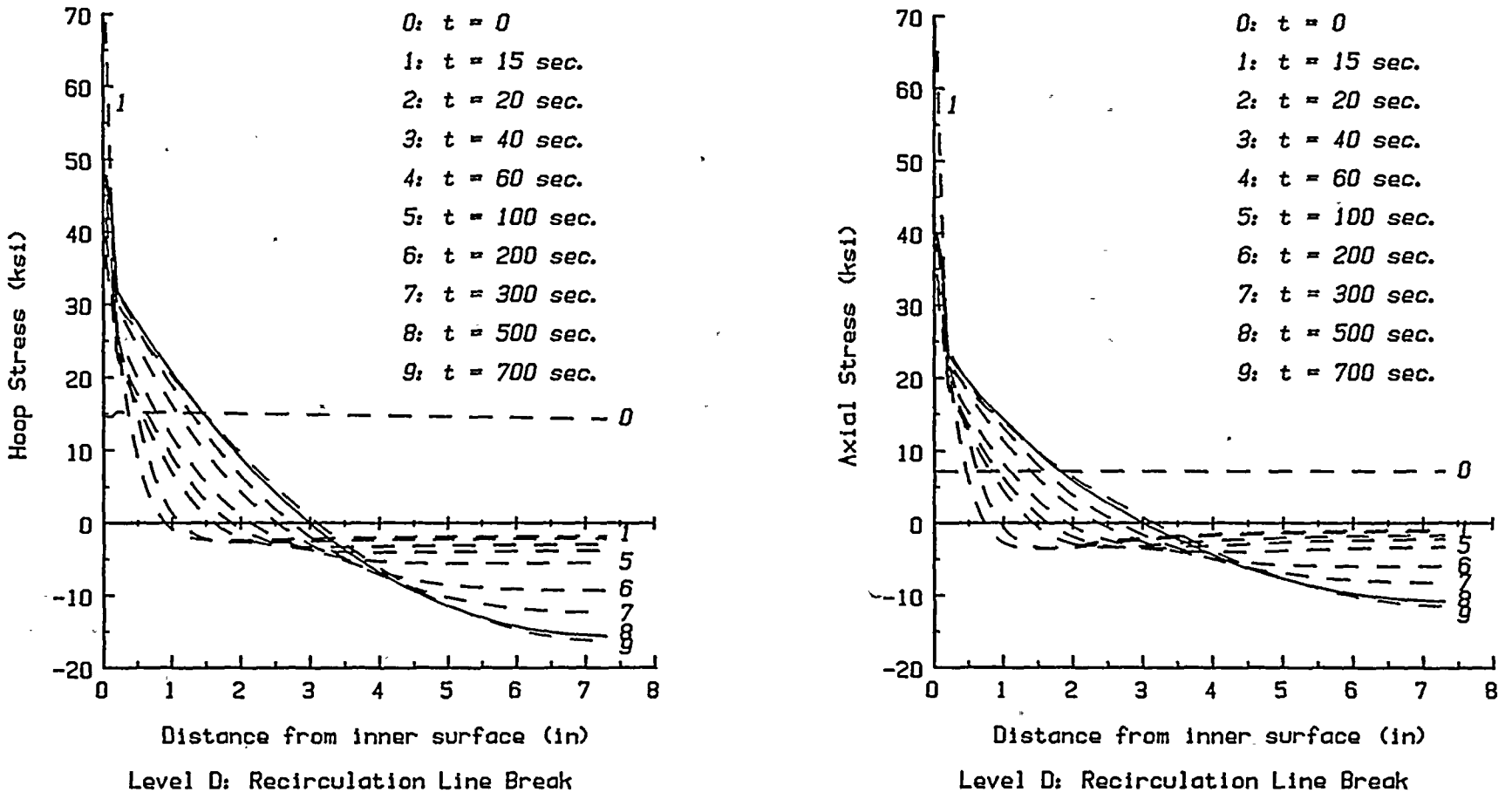

Figure 4-9
Axial and Circumferential Stress Distributions for Level D Recirculation Line Break for NMP-2

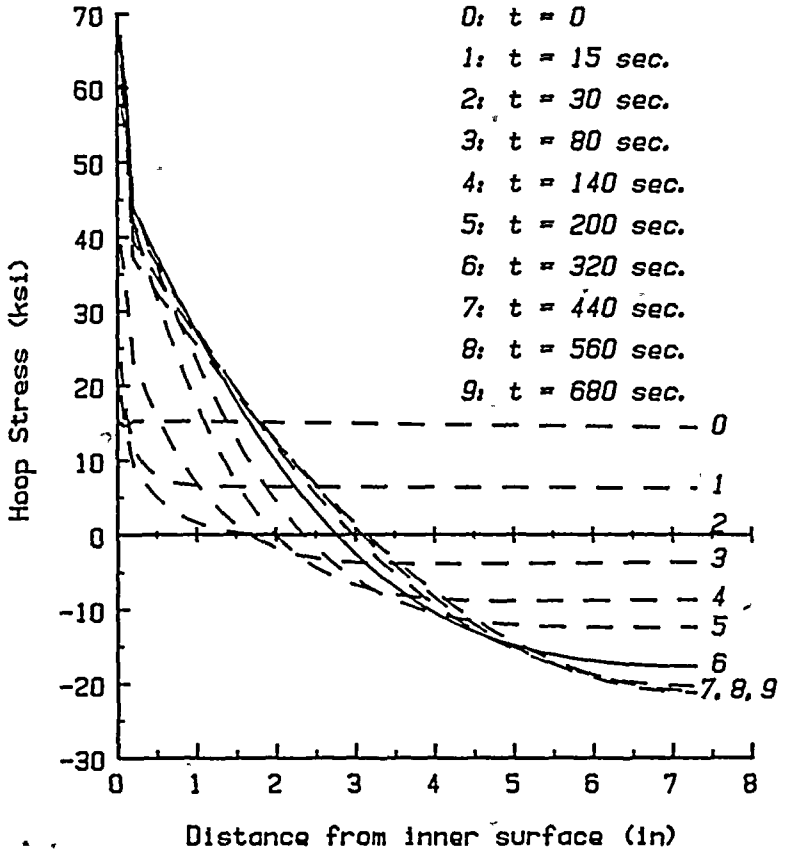

Level D: Recirculation Line Break NMP-1 DBA

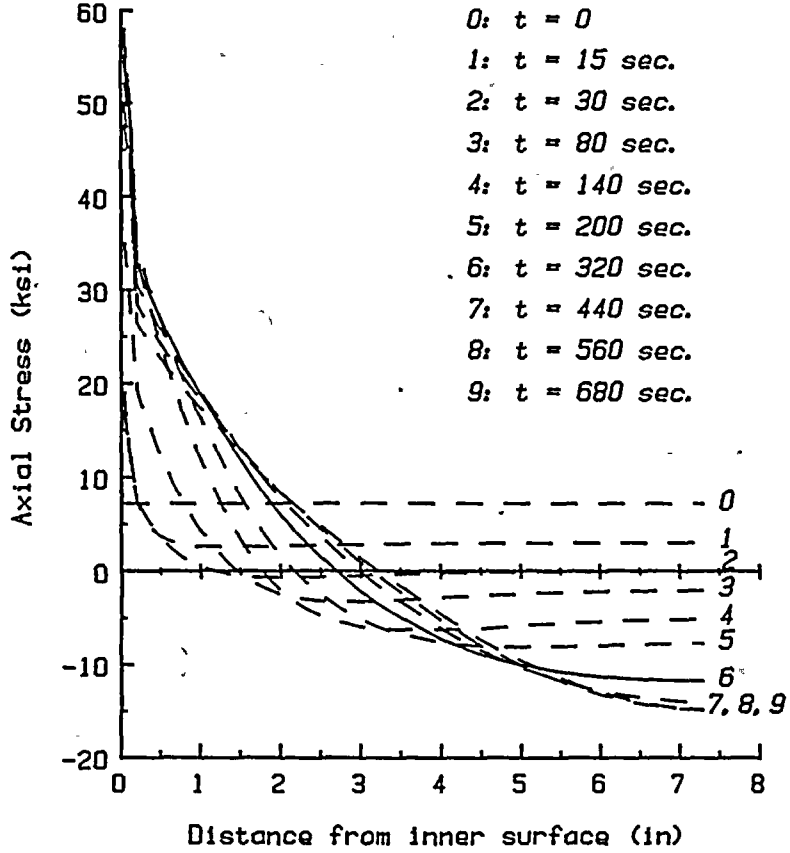

Level D: Recirculation Line Break NMP-1 DBA

Figure 4-10
Axial and Circumferential Stress Distributions for Level D Recirculation Line Break for NMP-1 DBA

5.0 Elastic-Plastic Fracture Mechanics Assessment

The limiting Level C and D transient loads were applied to a fracture mechanics model of the NMP-1 pressure vessel in accordance with the guidance provided in References [ASME92] and [WGFE92]. The USE™ (3.0) code package [USE93] was used to perform the calculations. A copy of the draft Appendix X [ASME92] is provided in Appendix A and the ASME Working Group on Flaw Evaluation draft stress intensity calculation procedure [WGFE92] is given in Appendix B.

5.1 Model Description

5.1.1 Vessel Geometry

The A302B material model used in the analysis was described in Section 2.0. In addition to the material model, USE™ (3.0) requires the following parameters:

Vessel Wall Thickness	=	7.281 in. (UFSAR Table V-1)
Vessel Inner Radius	=	106.344 in. (UFSAR Table V-1)
Vessel Clad Thickness	=	0.15625 in.
Crack Depth/Length Ratio	=	0.166667

5.1.2 Applied Loads

The results of the finite element calculations to determine the limiting Level C and D transients and loadings are described in Section 4.0. As a result of these calculations, the limiting Level C transient is the "NMP-1 Design Basis 250°F/7.5 min. Blowdown", and the limiting Level D transient is the "Steam Line Break". The limiting stress distribution was determined by examining the radial stress profiles at various times in the transient. As mentioned in Section 4.0, using stress distribution data at a time when the stresses are most severe for a one-inch crack may be slightly non-conservative when shorter cracks are considered. This small non-conservatism was circumvented by using an upper bound envelope of the actual stress distributions.

The limiting stress distributions were fit to a cubic polynomial using the guidance given in [WGFE92]. In order to provide good fits to the data, the base metal stresses were extrapolated to the ID surface. The remaining discontinuous component of the clad stresses are treated using a line load formulation as described in Section 5.1.4. The equivalent clad line loads are given in Table 5-1. The pressure acting along the crack surface was conservatively included in the clad line load. The fit to the base metal stress distribution is shown in Figures 5-1

through 5-4. Table 5-2 summarizes the stress distribution coefficients for use in the Appendix X analysis. The R-squared value for all of the fits is very close to unity which indicates accurate representation of the data.

5.1.3 Limits for Small Scale Yielding Analysis

As stated in Reference [ASME92], when the conditions fall in the category of elastic fracture mechanics with small-scale yielding, the J-integral may be calculated using crack-tip stress intensity formulae with plastic-zone correction. In order to estimate the limits of validity of the small-scale yielding assumption, an axially cracked cylindrical vessel with a radius to thickness ratio of 10, a wall thickness t=10 in., and a crack depth to thickness ratio a/t=0.25, was loaded by internal pressure and the resulting stress intensities were calculated. The effective crack depths were calculated using:

$$a_e = a_p + \frac{1}{6\pi}\left(\frac{K}{\sigma_{ys}}\right)^2$$

where,
a_e = effective crack size (in.)
a_p = physical crack depth (in.)
K = linear elastic stress intensity (ksi$\sqrt{}$in)
σ_{ys} = yield stress (ksi)

Two Ramberg-Osgood stress-strain models were analyzed: one with n=8.4 and alpha=2.6; the second with n=5.3 and alpha=7.2. The higher n-value case is more representative of the NMP-1 plates. The elastic calculations approximated pressure stresses by a linear distribution that matched the exact thick walled cylinder solution at the inner and outer surfaces. The plastic solution was calculated using the exact internal pressure induced stresses.

The results are summarized in Figure 5-5. The difference in solutions for small loads is due to the use of different elastic solution F factors in the two models. Based on this analysis, it is concluded that the small-scale yielding formulation is valid for stress intensity levels up to 100 ksi$\sqrt{}$in (J~335 in-lb/in^2) for an axial crack in a cylinder with an aspect ratio of 10. Since the calculated stress intensities for NMP-1 are well below 100 ksi$\sqrt{}$in., the small scale yielding analysis is appropriate for the NMP-1 vessel analysis.

5.1.4 Fracture Mechanics Model

The Reference [WGFE92] method for calculating stress intensities for surface flaws was used. A copy of the procedure proposed by the ASME Working Group on Flaw Evaluation is given in Appendix B. The procedure requires accurately fitting the stress distribution using the following polynomial fit:

$$\sigma = A_o + A_1X + A_2X^2 + A_3X^3 \qquad (5\text{-}1)$$

where,

A_i = regression constants
X = distance through the wall

The postulated flaw is a semi-elliptical surface crack with a surface length which is six times the depth. The stress intensity for the continuous component of the stresses was calculated from the following expression:

$$K_I^{CONTINUOUS} = [A_oG_o + A_1G_1a + A_2G_2a^2 + A_3G_3a^3]\sqrt{\pi a/Q} \qquad (5\text{-}2)$$

where,

a = crack depth

A_i = coefficients from Eq. 3-1 which represent the stress distribution over the crack ($0 \leq X \leq a$)

G_i = influence coefficients as a function of flaw aspect ratio and crack penetration (Appendix B)

Q = flaw shape parameter

$Q = 1 + 4.593\ (a/l)^{1.65} - q_y$

l = flaw surface length

q_y = plastic zone correction factor

$q_y = 0.212\ (A_o/\sigma_{ys})^2$

σ_{ys} = material yield stress

Since the slope of the stress distribution at the clad-base metal interface changes abruptly, the base metal stress distribution was extrapolated to the ID surface to provide an accurate fit over the postulated flaw depths. The Reference [TA73] linear elastic formulation was used to calculate the discontinuous component of the stress fields contribution to the crack tip stress intensity using:

$$K_I^{DISCONTINUOUS} = \frac{2P}{\sqrt{\pi a}} F(c/a, a/b) \qquad (5\text{-}3)$$

where,

$$F = \frac{3.52(1-c/a)}{(1-a/b)^{1.5}} - \frac{4.35-5.28c/a}{(1-a/b)^{0.5}} + \left(\frac{1.3-0.3(c/a)^{1.5}}{(1-(c/a)^2)^{0.5}} + 0.83-1.76c/a\right)(1-(1-c/a)a/b)$$

P = equivalent line load

a = flaw depth

b = wall thickness

c = load application position as measured from the ID surface

Equation 5-3 provides conservative estimates of the discontinuous stress component contribution of the total stress intensity since the formulation is for an infinite crack length. Since Eq. (3-3) is a linear elastic equation, the small scale yielding correction was applied:

$$a_e = a + \left(\frac{1}{6\pi}\right)\left(\frac{K}{\sigma_{ys}}\right)^2 \qquad (5\text{-}4)$$

where,

a = physical crack depth

a_e = effective crack depth

In order to simplify the computer algorithm and to ensure conservative results, the small scale yielding correction was applied to both the cladding and base metal stress intensity factors. This approach yields very conservative results since the flaw shape parameter in equation 5-2 includes a plastic zone correction factor. The total stress intensity factor was obtained by superposition:

$$K = K_I^{CONTINUOUS} + K_I^{DISCONTINUOUS} \qquad (5\text{-}5)$$

In accordance with Reference [ASME92], a spectrum of initial flaws, up to 1/10 of the base metal wall thickness, were assumed. The smallest flaw assumed was 0.05 in., and the postulated flaws were increased in size by increments of 0.05 in., up to a maximum flaw depth of 0.75 in.

5.2 Calculations for A302B Material Model

The pointwise input model was used for the A302B material model calculations. Using this model, the J-R curve is assumed flat after the initial 0.1 in. of crack extension. The G-8-1 plate was analyzed using the A302B material model since it is the limiting plate from a ductile fracture perspective (Reference [MA93]).

5.2.1 Level C Loading

The results of the calculations for the Level C loading have shown that the limiting flaw orientation is the axial flaw. For initial base metal flaw depths of up to 1/10 of the vessel wall thickness, the ASME Appendix X criteria are satisfied at USE levels as low as 10 ft-lbs. In all cases, the largest applied-J values for the flaw growth of 0.1 in. criterion are obtained at the deepest initial postulated flaw depth. The results for the Level C analysis are summarized in Table 5-3 for the axial flaw.

5.2.2 Level D Loading Analysis

The results of the calculations for the Level D loading also show that the limiting flaw orientation is the axial flaw. For initial base metal flaw depths of up to 1/10 of the vessel wall thickness, the ASME Appendix X criteria are satisfied at USE levels as low as 20 ft-lbs. The results for the Level D analysis are summarized in Table 5-4 for the axial flaw.

5.2.3 Tensile Instability Analysis

Based on the analysis performed, the deepest flaw during the most severe Level C or D transient is less than 1.2 inches. Conservatively assuming the flaw extends completely around the circumference, and using the finite element stress profiles, the remaining ligament will experience stresses well below the yield strength and is therefore safe in terms of tensile instability.

Table 5-1

NMP-1 Clad Stresses

Case	Extrapolated Surface Stress (ksi)	Clad Stress Minus Extrapolated Surface Stress (ksi)	Residual Stress (ksi)	Clad Total Stress (ksi)	Crack Surface Pressure (ksi)	Clad Equivalent Line Stress (kp/in)
Hoop-Level C	45.207	16.557	20.6	37.157	1.05	6.856
Axial-Level C	35.264	16.790	20.0	36.790	1.05	6.798
Hoop-Level D	58.690	19.886	20.6	40.486	1.05	7.376
Axial-Level D	45.476	21.377	20.0	41.377	1.05	7.515

Table 5-2
Base Metal Stress Distribution Coefficients

	A_o	A_1	A_2	A_3
Level C-- Hoop	45.165	-22.335	2.571	0.228
Level C - Axial	35.294	-25.420	9.941	-2.183
Level D - Hoop	58.791	-33.934	7.967	-1.052
Level D - Axial	45.651	-33.636	12.136	-2.263

Table 5-3
Comparison of Applied Loads with ASME Criteria for
Level C Loading Conditions and an Axial Flaw Orientation[1]

USE Level	Δa=0.1 Criterion: Applied J (in-lb/in^2)	Δa=0.1 Criterion: Material $J_{0.1}$ (in-lb/in^2)	Flaw Stability Criterion: Applied T	Flaw Stability Criterion: Material T	Criteria Satisfied
10	183	199	<0.5	2.6	yes
20	183	230	<0.5	3.7	yes
30	183	261	<0.5	7.3	yes
40	183	292	<0.5	13.2	yes
50	183	323	<0.5	18.3	yes
60	183	353	---	--	yes, $J_{app}<J_{IC}$
70	183	384	---	--	yes, $J_{app}<J_{IC}$
80	183	438	---	--	yes, $J_{app}<J_{IC}$
90	183	517	---	--	yes, $J_{app}<J_{IC}$
100	183	597	---	--	yes, $J_{app}<J_{IC}$

[1] Results shown are for the most limiting initial flaw over the spectrum of flaws analyzed

Table 5-4
Comparison of Applied Loads with ASME Criteria for
Level D Loading Conditions and an Axial Flaw Orientation [1]

USE Level	Flaw Stability Criterion		Criteria
	Applied T	Material T	Satisfied
10	$J_{app}>J_{MAX}$	--	no
20	<0.8	11.0	yes
30	<0.8	18.3	yes
40	--	--	yes, $J_{app}<J_{IC}$
50	--	--	yes, $J_{app}<J_{IC}$
60	--	--	yes, $J_{app}<J_{IC}$
70	--	--	yes, $J_{app}<J_{IC}$
80	--	--	yes, $J_{app}<J_{IC}$
90	--	--	yes, $J_{app}<J_{IC}$
100	--	--	yes, $J_{app}<J_{IC}$

[1] Results shown are for the most limiting initial flaw over the spectrum of flaws analyzed.

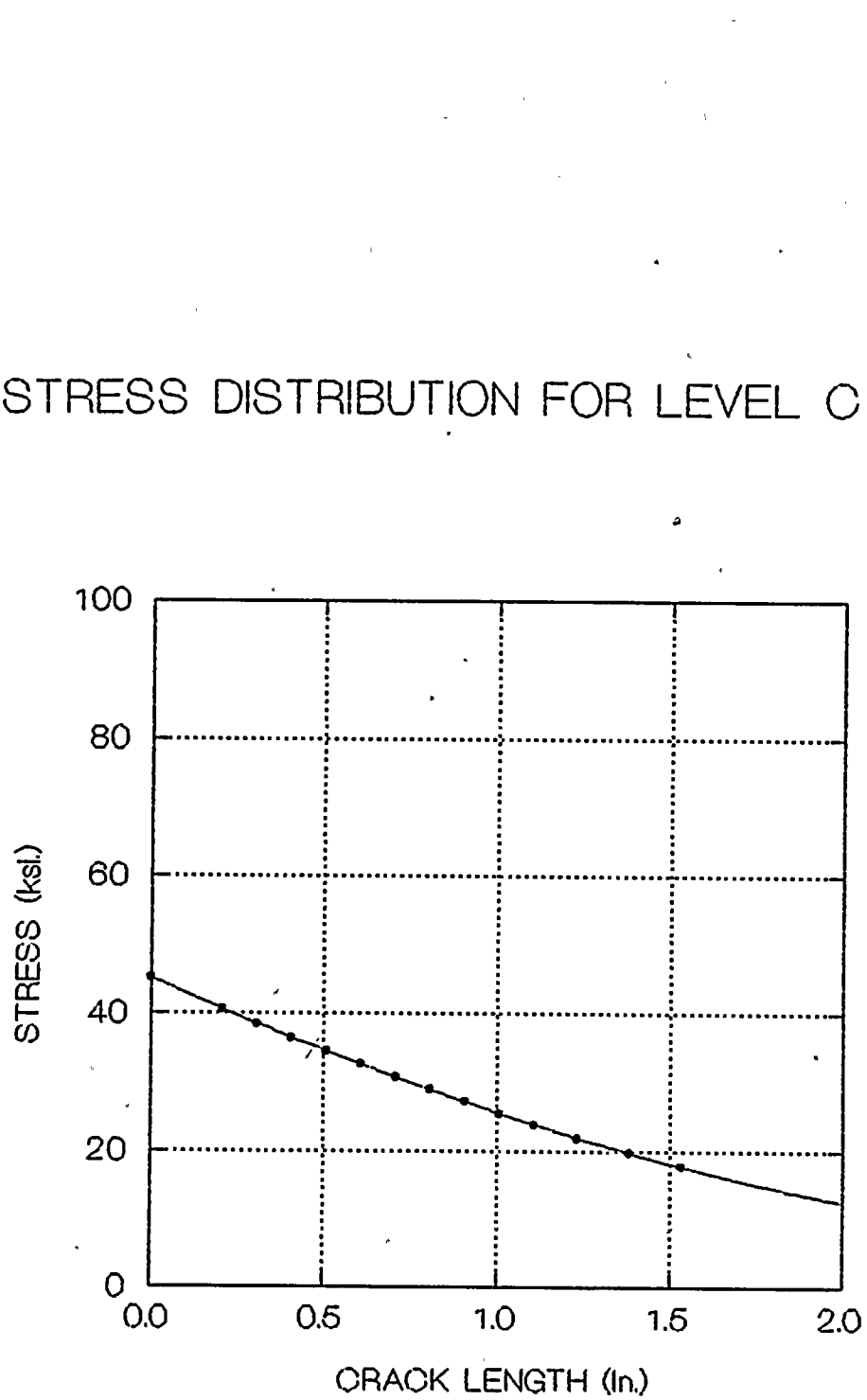

Figure 5-1
Peak Circumferential Base Metal Stress Distribution for
NMP-1 Design Basis 250°F/7.5 Min. Blowdown Transient

AXIAL STRESS DISTRIBUTION FOR LEVEL C TRANSIENT

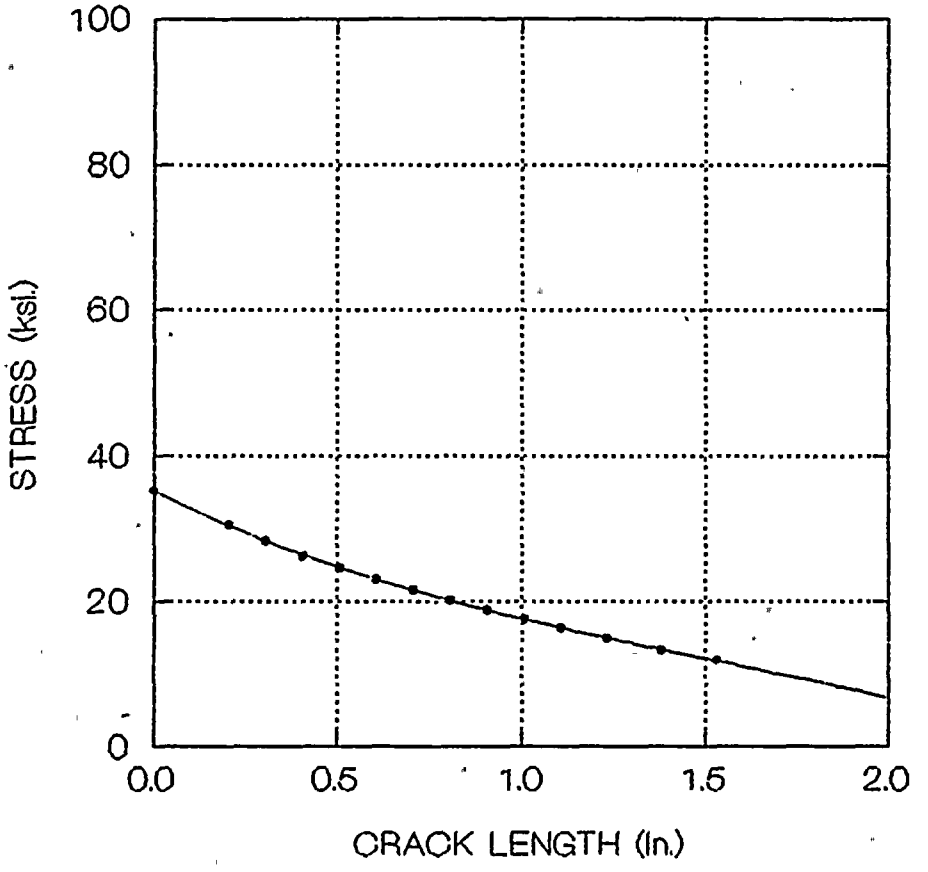

Figure 5-2
Peak Axial Base Metal Stress Distribution for
NMP-1 Design Basis 250°F/7.5 Min. Blowdown Transient

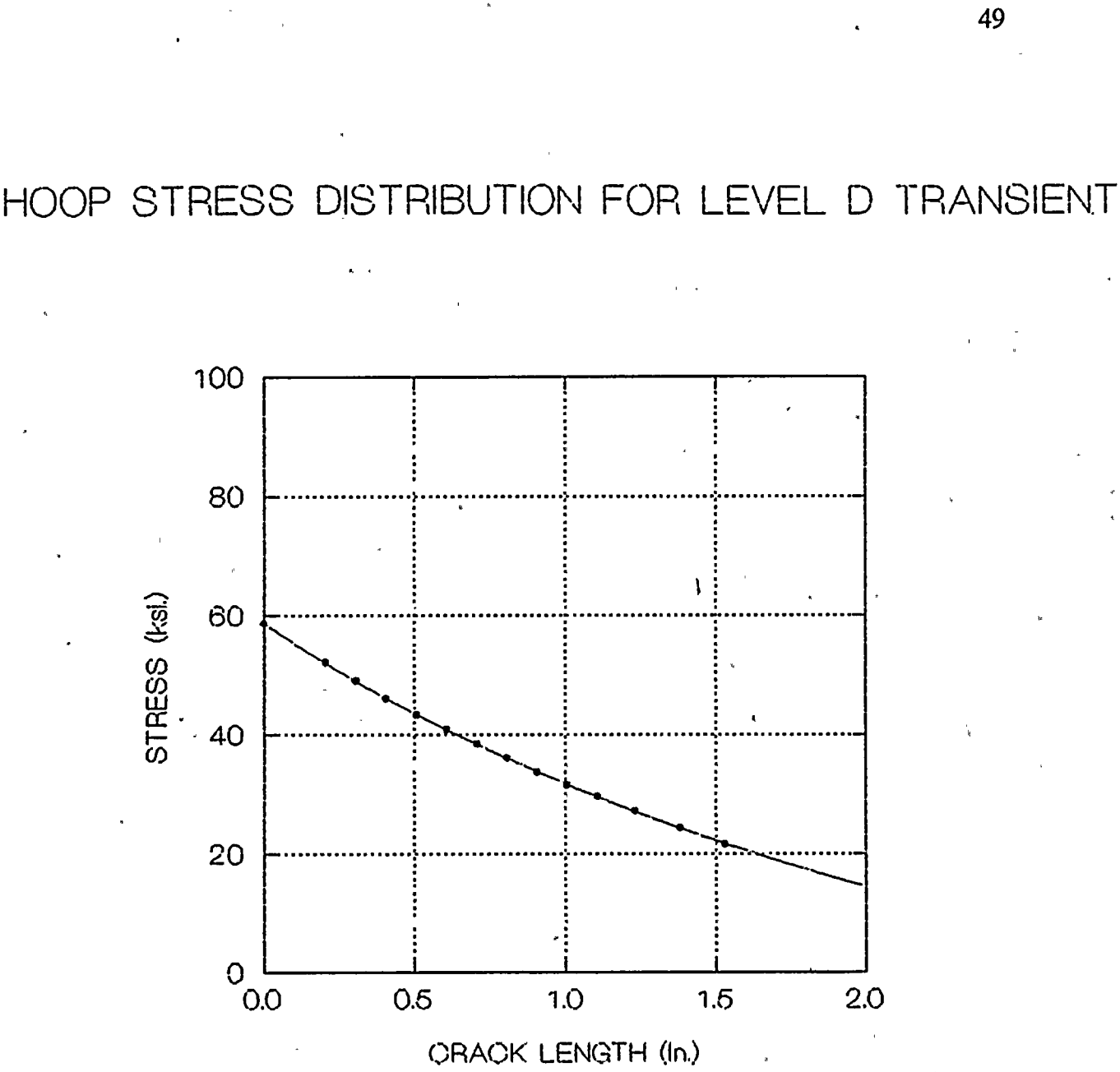

Figure 5-3
Peak Circumferential Base Metal Stress Distribution for
Steam Line Break Transient

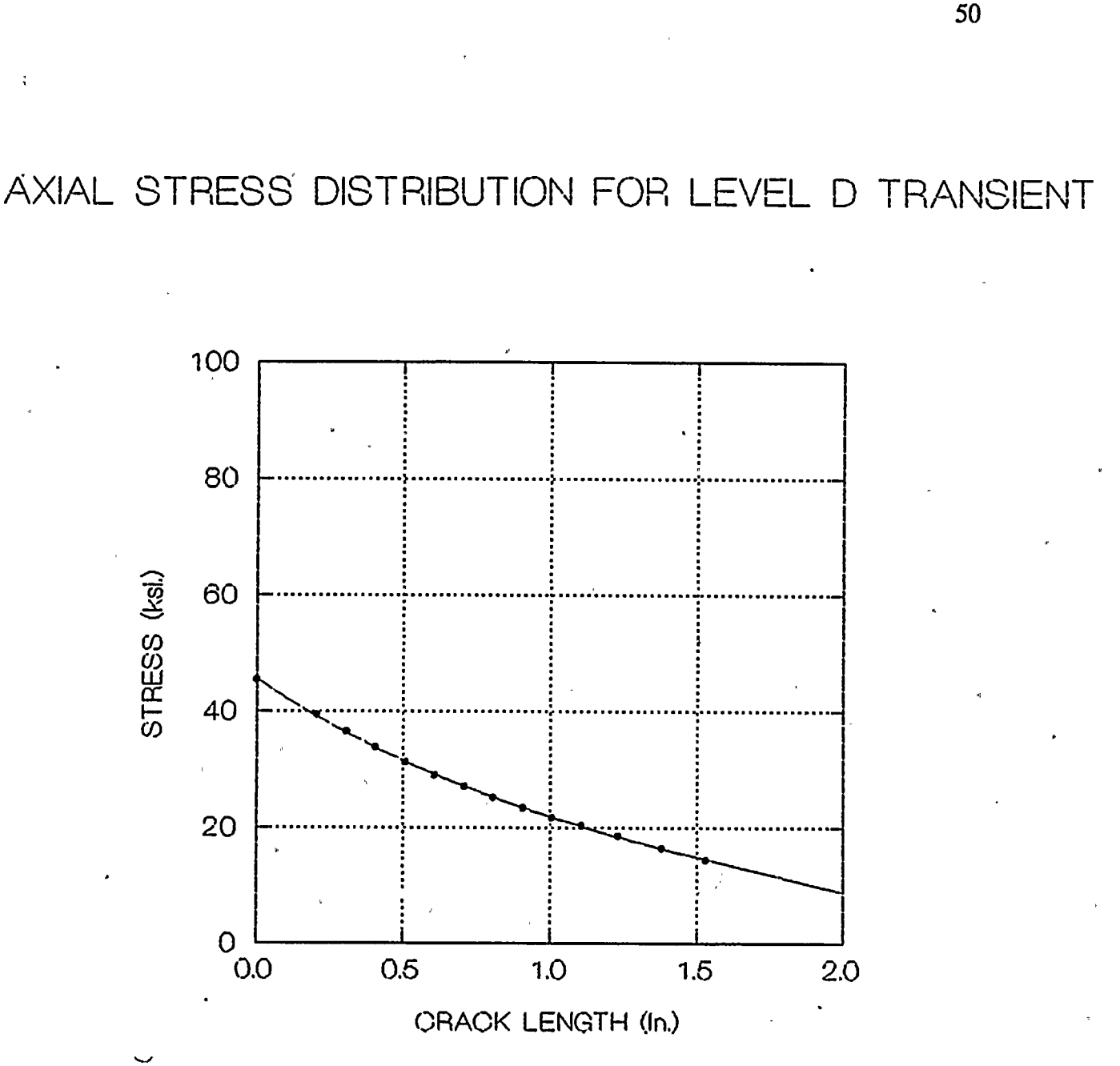

Figure 5-4
Peak Axial Base Metal Stress Distribution for
Steam Line Break Transient

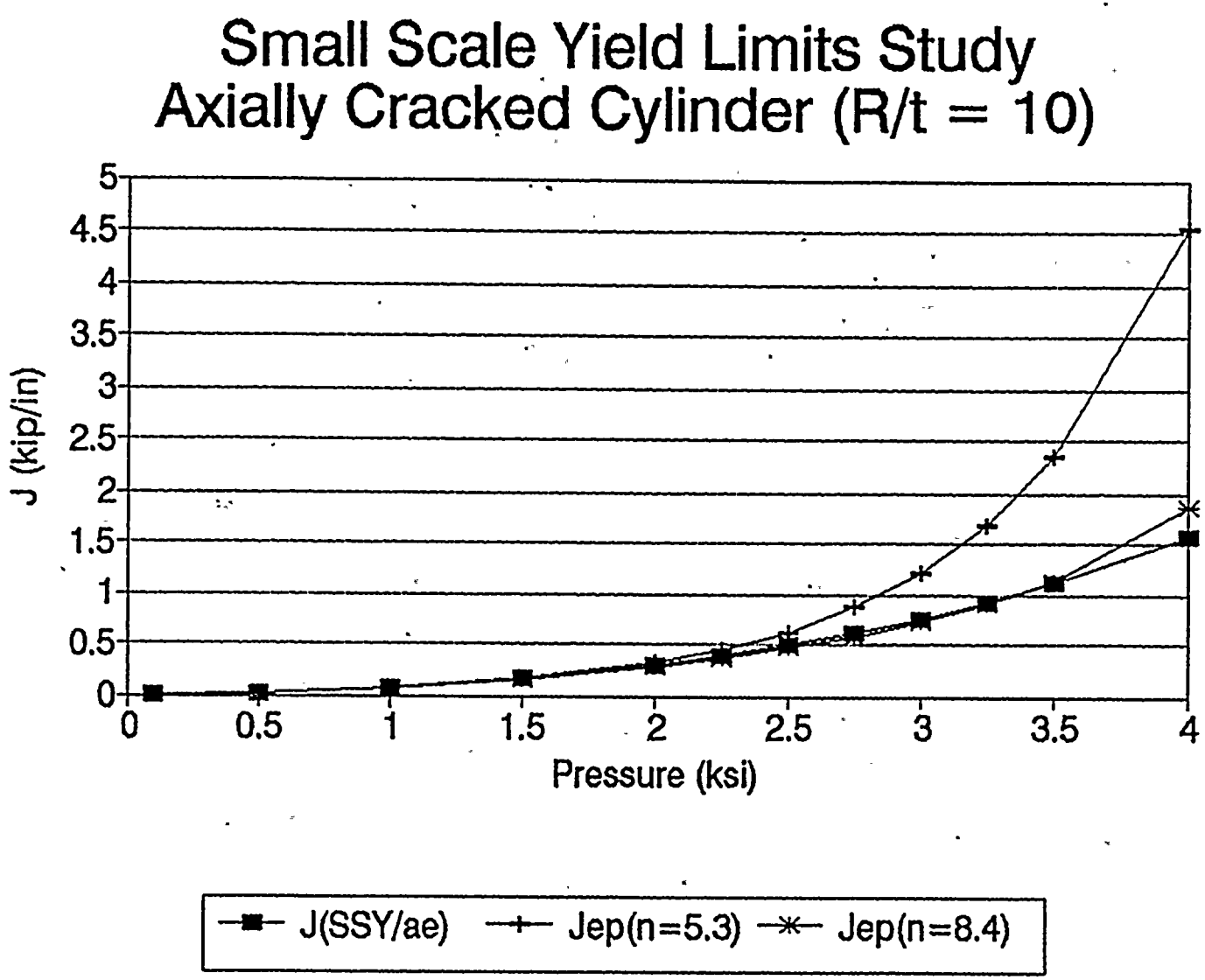

Figure 5-5
Comparison Between Small Scale Yielding Solution (J(SSY/ae)) and the Elastic-Plastic Solutions with Hardening Exponents of 5.3 (Jep(n=5.3)) and 8.4 (Jep(n=8.4))

6.0 Summary and Conclusions

The results of the elastic-plastic fracture mechanics assessment are shown in Table 6-1. As discussed in Reference [MA93], the A302B material model best represents the NMP-1 beltline plates. The A302B material model, applied to the case of an axial flaw orientation, yields the most conservative results. Based on the calculations reported in Reference [MA93] and herein, it has been concluded that the NMP-1 plate G-8-1 is limiting from a ductile fracture perspective, and the USE must be maintained above 23 ft-lbs. Based on the data reported in Reference [MA93], none of the NMP-1 beltline plates are expected to fall below the 23 ft-lb level. Although the Appendix X criteria are satisfied at or above the 23 ft-lb level, it is not clear that the plant should be operated at this ductility level. It is anticipated that future federally funded research and subsequent regulations will address this issue.

Table 6-1

Minimum Upper Shelf Energy Level for NMP-1 Plates
Based on the ASME Draft Appendix X Evaluation Criteria
for Service Levels A, B, C and D

Plate	ASME Service Level A&B	Material Model	Minimum USE (Ft-Lbs)	
			Flaw Growth of 0.1 in. Criterion $J_1 < J_{0.1}$	Flaw Stability Criterion
G-8-1	A&B	A302B	13	23
G-307-4	A&B	A302B	13	23
G-8-1	C	A302B	10	10
G-8-1	D	A302B	n/a	20

7.0 References

[ASME92] ASME Draft Code Case N-XXX, "Assessment of Reactor Vessels with Low Upper Shelf Charpy Energy Levels", Revision 11, May 27, 1992.

[CENC] Unit 1 Analytical Report for Niagara Mohawk Reactor Vessel, Report No. CENC 1142, ACC No. 002301187, Appendix B Thermal Analysis.

[FSAR] Updated FSAR Volume IV, Section I, Page I-11.

[HI89] Hiser, A.L., Terrell, J.B., "Size Effects on J-R Curves for A302B Plate", NUREG/CR-5265, January, 1989.

[MA92] Manahan, M.P., Soong, Y., "Response to NRC General Letter 92-01 for Nine Mile Point Unit 1", NMPC Project 03-9425, June 12, 1992.

[MA93] Manahan, M.P., Final Report to NRC, "Elastic-Plastic Fracture Mechanics Assessment of Nine Mile Point Unit 1 Beltline Plates for Service Level A and B Loadings", February 19, 1993.

[NEDC] NEDC-31446P, NMP-1 SAFER/CORECOOL/GESTR-LOCA Loss of Coolant Accident Analysis.

[NMP1DP] NMP-1 Drywell Pressure Calculation, SO-TORUS-M009, GENE-770-91-34.

[NMP2TC] NMP-2, 762E673, Reactor Vessel Thermal Cycles.

[STRS] Section E9, Emergency & Faulted Analysis of Recirculation Outlet Nozzle 251" BWR Vessel. STRS 16.010-5039A, page E11, 12. Unit 2 Stress Analysis.

[TA73] Tada, H., Paris, P.C., Irwin, G.R., "The Stress Analysis of Cracks Handbook", Del Research Corp., 1973.

[TCD] Unit 2 Reactor Vessel Thermal Cycles Diagram 762E673.

[TRUMP] Manahan, M.P., "TRUMP/MPM: Thermal Transient Heat Transfer Analysis Code, Version 1.0, September, 1989.

[USE93] USE™ (3.0)Code Package for Elastic-Plastic Fracture Mechanics Assessment of Nuclear Reactor Pressure Vessels, MPM Research & Consulting, ©1993.

[WELD3] "WELD3 Computer Code Verification", MPM Research & Consulting, Calculation No. MPM-NMPC-99205, Rev. 0, January 21, 1993.

[WGFE92] ASME Working Group on Flaw Evaluation, Proposed Changes to Article A-3000 entitled, "Method for K_I Determination", August, 1992.

Acknowledgement

Dr. Randall B. Stonesifer of Computational Mechanics, Inc. performed all of the finite element analyses and provided many valuable suggestions related to the fracture mechanics model.

Appendices

Appendix A

ASME Draft Appendix X

"Assessment of Reactor Vessels with Low Upper Shelf Charpy Energy Levels"

DRAFT

CODE CASE N-XXX

ASSESSMENT OF REACTOR VESSELS WITH LOW UPPER SHELF CHARPY ENERGY LEVELS

May 27, 1992

REVISION 11

DRAFT HISTORY

REVISION	0	AUGUST 25, 1987
REVISION	1	JANUARY 19, 1988
REVISION	2	APRIL 19, 1988
REVISION	3	AUGUST 30, 1988
REVISION	4	NOVEMBER 30, 1988
REVISION	5	FEBRUARY 27, 1989
REVISION	6	JANUARY 5, 1990
REVISION	7	APRIL 12, 1990
REVISION	8	JANUARY 10, 1991
REVISION	8 - MARKED COPY	APRIL 15, 1991
REVISION	9	JANUARY 17, 1992
REVISION	10	APRIL 17, 1992
REVISION	11	CURRENT

ASSESSMENT OF REACTOR VESSELS WITH LOW UPPER SHELF CHARPY ENERGY LEVELS

TABLE OF CONTENTS

Case N-XXX
Assessment of Reactor Vessels With Low Upper Shelf Charpy Energy Levels
Section XI, Division 1

Inquiry: Section XI, Division 1, IWB-3730, requires that during reactor operation, load and temperature conditions shall be maintained to provide protection against failure due to the presence of postulated flaws in the ferritic portions of the reactor coolant pressure boundary. Under Section XI, Division 1, what procedure may be used to evaluate a reactor vessel with a low upper shelf Charpy impact energy level as defined in ASTM E 185-82 to demonstrate integrity for continued service at upper shelf conditions?

Reply: It is the opinion of the Committee that a reactor vessel with a low upper shelf Charpy impact energy level may be evaluated to demonstrate integrity for continued service for upper shelf conditions in accordance with the following.

1.0 EVALUATION PROCEDURES AND ACCEPTANCE CRITERIA

Section XI, Division 1, Appendix G, "Fracture Toughness Criteria for Protection Against Failure", provides analytical procedures based on the principles of linear-elastic fracture mechanics that may be used to define load and temperature conditions to provide protection against nonductile failure due to the presence of postulated flaws in the ferritic portions of the reactor coolant pressure boundary. To prevent ductile failure of a reactor vessel with a low upper shelf Charpy impact energy level the vessel shall be evaluated using the principles of elastic-plastic fracture mechanics. Flaws shall be postulated in the reactor vessel at locations of predicted low upper shelf Charpy impact energy and the applied J-integral for these flaws shall be calculated and compared with the J-integral fracture resistance of the material to determine acceptability. Factors of safety on applied load for limited ductile flaw growth, and on flaw stability due to ductile tearing, shall be satisfied. All specified design transients for the reactor vessel shall be considered. Evaluation procedures and acceptance criteria based on the principles of elastic-plastic fracture mechanics are given in Appendix A of this Code Case.

The evaluation shall be the responsibility of the Owner and shall be subject to review by the regulatory and enforcement authorities having jurisdiction at the plant site.

APPENDIX A TO CODE CASE N-XXX

ASSESSMENT OF REACTOR VESSELS WITH LOW UPPER SHELF CHARPY ENERGY LEVELS

ARTICLE A-1000

INTRODUCTION

A-1100 SCOPE

This Appendix provides acceptance criteria and evaluation procedures for determining the acceptability for operation of a reactor vessel when the vessel metal temperature is in the upper shelf range. The methodology is based on the principles of elastic-plastic fracture mechanics. Flaws are postulated in the reactor vessel at locations of predicted low upper shelf Charpy impact energy and the applied J-integral for these flaws is calculated and compared with the J-integral fracture resistance of the material to determine acceptability. All specified design transients for the reactor vessel shall be considered.

A-1200 PROCEDURE OVERVIEW

The following is a summary of the analytical procedure which may be used.

(a) Postulate flaws in the reactor vessel according to the criteria in A-2000.

(b) Determine the loading conditions at the location of the postulated flaws for Level A, B, C and D Service loadings.

(c) Obtain the material properties, including E, σ_y, and the J-integral resistance curve (J-R curve), at the locations of the postulated flaws. Requirements for determining the J-R curve are given in A-3300.

(d) Evaluate the postulated flaws according to the acceptance criteria in A-2000. Requirements for evaluating the applied J-integral are given in A-3200, and for determining flaw stability in A-3400. Three permissible evaluation approaches are described in A-3500. Detailed calculation procedures for Level A and B Service loadings are given in A-4000.

A-1300 GENERAL NOMENCLATURE

a	=	flaw depth which includes ductile flaw growth	(in.)
a_e	=	effective flaw depth which includes ductile flaw growth and a plastic-zone correction	(in.)
a_e^*	=	effective flaw depth at flaw instability, which includes ductile flaw growth and a plastic-zone correction	(in.)
a_o	=	postulated initial flaw depth	(in.)
Δa	=	amount of ductile flaw growth	(in.)
Δa^*	=	amount of ductile flaw growth at flaw instability	(in.)
C_1, C_2	=	material constants used to describe the power-law fit to the J-integral resistance curve for the material, $J_R = C_1(\Delta a)^{C_2}$	
(CR)	=	cooldown rate	(°F/hour)
E	=	Young's modulus	(ksi)
E'	=	$E/(1-\upsilon^2)$	(ksi)
F_1, F_2, F_3	=	geometry factors used to calculate the stress intensity factor	(dimensionless)
F_1^*, F_2^*, F_3^*	=	geometry factors used to calculate the stress intensity factor at flaw instability	(dimensionless)
J	=	J-integral due to the applied loads	(in.-lb/in.^{2})
J_R	=	J-integral fracture resistance for the material	(in.-lb/in.^{2})

$J_{0.1}$	=	J-integral fracture resistance for the material at a ductile flaw growth of 0.10 in.	(in.-lb/in.^{2})
J_I	=	applied J-integral at a flaw depth of a_o + 0.10 in.	(in.-lb/in.^{2})
J^*	=	J-integral at flaw instability	(in.-lb/in.^{2})
K_I	=	mode I stress intensity factor	(ksi $\sqrt{\text{in.}}$)
K_{Ip}	=	mode I stress intensity factor due to internal pressure, calculated with no plastic-zone correction	(ksi $\sqrt{\text{in.}}$)
K'_{Ip}	=	K_{Ip} calculated with a plastic-zone correction	(ksi $\sqrt{\text{in.}}$)
K^*_{Ip}	=	K_{Ip} at flaw instability, calculated with a plastic-zone correction	(ksi $\sqrt{\text{in.}}$)
K_{It}	=	mode I stress intensity factor due to a radial thermal gradient through the vessel wall, calculated with no plastic-zone correction	(ksi $\sqrt{\text{in.}}$)
K'_{It}	=	K_{It} calculated with a plastic-zone correction	(ksi $\sqrt{\text{in.}}$)
K^*_{It}	=	K_{It} at flaw instability, calculated with a plastic-zone correction	(ksi $\sqrt{\text{in.}}$)
K_r	=	ordinate of the failure assessment diagram curve	(dimensionless)
K'_r	=	ratio of the stress intensity factor to the fracture toughness for the material	(dimensionless)
p	=	internal pressure	(ksi)
p_a	=	accumulation pressure as defined in the plant-specific Overpressure Protection Report, but not exceeding 1.1 times the design pressure	(ksi)

p_a	=	pressure used to calculate the applied J-integral/tearing modulus line	(ksi)
p^*	=	internal pressure at flaw instability	(ksi)
p_o	=	reference limit-load internal pressure	(ksi)
R_i	=	inner radius of the vessel	(in.)
S_r	=	abscissa of the failure assessment diagram curve	(dimensionless)
S_r'	=	ratio of internal pressure to reference limit-load internal pressure	(dimensionless)
(SF)	=	safety factor	(dimensionless)
t	=	vessel wall thickness	(in.)
T	=	tearing modulus due to the applied loads	(dimensionless)
T_R	=	tearing modulus resistance for the material	(dimensionless)
W	=	parameter used to relate the applied J-integral to the applied tearing modulus	(dimensionless)
υ	=	Poisson's ratio	(dimensionless)
σ_f	=	reference flow stress, specified as 85 ksi	(ksi)
σ_y	=	yield strength for the material	(ksi)

ARTICLE A-2000

ACCEPTANCE CRITERIA

The adequacy of the upper shelf toughness of the reactor vessel shall be determined by analysis. The reactor vessel is acceptable for continued service when the criteria of Paragraphs (a), (b), and (c) are satisfied.

(a) Level A and B Service Loadings

When evaluating the adequacy of the upper shelf toughness for the weld material for Level A and B Service loadings, postulate an interior semi-elliptical surface flaw with a depth one-quarter of the wall thickness and a length six times the depth, with the flaw's major axis oriented along the weld of concern and the flaw plane oriented in the radial direction. When evaluating the adequacy of the upper shelf toughness for the base material, postulate both interior axial and circumferential flaws with depths one-quarter of the wall thickness and lengths six times the depth and use the toughness properties for the corresponding orientation. Smaller flaw sizes may be used on an individual case basis when justified. Two criteria shall be satisfied:

(1) The applied J-integral evaluated at a pressure which is 1.15 times the accumulation pressure as defined in the plant-specific Overpressure Protection Report, with a factor of safety of 1.0 on thermal loading for the plant specified heatup and cooldown conditions, shall be shown to be less than the J-integral characteristic of the material resistance to ductile tearing at a flaw growth of 0.10 in.

(2) The flaw shall be shown to be stable, with the possibility of ductile flaw growth, at a pressure which is 1.25 times the accumulation pressure defined in Subparagraph (1), with a factor of safety of 1.0 on thermal loading for the plant specified heatup and cooldown conditions.

The J-integral resistance versus crack growth curve shall be a conservative representation for the vessel material under evaluation.

(b) Level C Service Loadings

When evaluating the adequacy of the upper shelf toughness for the weld material for Level C Service loadings, postulate interior semi-elliptical surface flaws with depths up to 1/10 of the base metal wall thickness, plus the cladding thickness, with total depths not to exceed 1.0 in., and a surface length six times the depth, with the flaw's major axis oriented along the weld of concern and the flaw plane oriented in the radial direction. When evaluating the adequacy of the upper shelf toughness for the base material, postulate both interior axial and circumferential flaws, and use the toughness properties for the corresponding orientation. Flaws of various depths, ranging up to the maximum postulated depth, shall be analyzed to determine the most limiting flaw depth. Smaller maximum flaw sizes may be used on an individual case basis when justified. Two criteria shall be satisfied:

(1) The applied J-integral shall be shown to be less than the J-integral characteristic of the material resistance to ductile tearing at a flaw growth of 0.10 in., using a factor of safety of 1.0 on loading.

(2) The flaws shall be shown to be stable, with the possibility of ductile flaw growth, using a factor of safety of 1.0 on loading.

The J-integral resistance versus crack growth curve shall be a conservative representation for the vessel material under evaluation.

(c) Level D Service Loadings

When evaluating the adequacy of the upper shelf toughness for Level D Service loadings, postulate flaws as specified for Level C Service loadings in Paragraph b), and use the toughness properties for the corresponding orientation. Flaws of various depths, ranging up to the maximum postulated depth, shall be analyzed to determine the most limiting flaw depth. Smaller maximum flaw sizes may be used on an individual case basis when justified. The flaws shall be shown to be stable, with the possibility of ductile flaw growth, using a factor of safety of 1.0 on loading. The J-integral resistance versus crack growth curve shall be a best estimate representation for the vessel material under evaluation.

The stable flaw depth shall not exceed 75% of the vessel wall thickness, and the remaining ligament shall be safe from tensile instability.

ARTICLE A-3000

ANALYSIS

A-3100 SCOPE

This Article contains a general description of procedures which shall be used to evaluate the applied fracture mechanics parameters, as well as requirements for selecting the J-R curve for the material. References are made to acceptable approaches to apply the criteria.

A-3200 APPLIED J-INTEGRAL

The calculation of the J-integral due to the applied loads shall account for the full elastic-plastic behavior of the stress-strain curve for the material. When the conditions fall into the category of elastic fracture mechanics with small-scale yielding, the J-integral may alternately be calculated by using crack-tip stress intensity factor formulae with a plastic-zone correction. The method of calculation shall be validated and documented.

A-3300 SELECTION OF THE J-INTEGRAL RESISTANCE CURVE

When evaluating the vessel for Level A, B and C Service loadings, the J-integral resistance versus crack growth curve (J-R curve) shall be a conservative representation of the toughness of the controlling beltline material at upper shelf temperatures in the operating range. When evaluating the vessel for Level D Service loadings, the J-R curve shall be a best estimate representation of the toughness of the controlling beltline material at upper shelf temperatures in the operating range. One of the following options shall be used to determine the J-R curve.

(a) A J-R curve generated for the actual material under consideration by following accepted test procedures may be used. The J-R curve shall be based on the proper combination of crack orientation, temperature and fluence level. The crack growth shall include ductile tearing with no occurrence of cleavage.

(b) A J-R curve generated from a J-integral database obtained from the same class of material under consideration with the same orientation using appropriate correlations for the effects of temperature, chemical composition and fluence level may be used. The crack growth shall include ductile tearing with no occurrence of cleavage.

(c) When the approaches of (a) or (b) are not possible, indirect methods of estimating the J-R curve may be used provided these methods are justified for the material under consideration.

A-3400 FLAW STABILITY

The equilibrium equation for stable flaw growth is

$$J = J_R$$

where J is the J-integral due to the applied loads for the postulated flaw in the vessel, and J_R is the J-integral resistance to ductile tearing for the material.

The inequality for flaw stability due to ductile tearing is

$$\frac{\partial J}{\partial a} < \frac{dJ_R}{da}$$

where $\partial J/\partial a$ is the partial derivative of the applied J-integral with respect to the flaw depth a with load held constant, and dJ_R/da is the slope of the J-R curve. Under a condition of increasing load, stable flaw growth will continue as long as $\partial J/\partial a$ remains less than dJ_R/da.

A-3500 EVALUATION APPROACH FOR LEVEL A AND B SERVICE LOADINGS

The procedure given in A-4200 shall be used to evaluate the applied J-integral for a specified amount of ductile flaw growth.

There are three approaches that are equally acceptable for applying the flaw stability acceptance criteria according to the governing flaw stability rules in A-3400. The first is a J-R curve - crack driving force diagram approach. In this approach flaw stability is evaluated by a direct application of the flaw stability rules given in A-3400. Guidelines for using this approach are given in A-4310. The second is a failure assessment diagram approach. A procedure based on this approach for the

postulated initial one-quarter wall thickness flaw is given in A-4320. The third is a J-integral/tearing modulus approach. A procedure based on this approach for the postulated initial one-quarter wall thickness flaw is given in A-4330.

ARTICLE A-4000

EVALUATION PROCEDURES FOR LEVEL A AND B SERVICE LOADINGS

A-4100 SCOPE

This Article contains calculation procedures to be used to satisfy the acceptance criteria in A-2000 for Level A and B Service loadings. A procedure to be used to satisfy the J-integral criterion for a specified amount of flaw growth of 0.10 in. is given in A-4200. Procedures to satisfy the flaw stability criterion are given in A-4300. These procedures include the axial and circumferential flaw orientations.

A-4200 EVALUATION PROCEDURE FOR THE APPLIED J-INTEGRAL

A-4210 CALCULATION OF THE APPLIED J-INTEGRAL

The calculation of the applied J-integral consists of two steps: Step 1 is to calculate the effective flaw depth which includes a plastic-zone correction; and Step 2 is to calculate the J-integral for small-scale yielding based on this effective flaw depth.

Step 1

For an axial flaw with a depth a, calculate the stress intensity factor due to internal pressure with a safety factor (SF) on pressure by using

$$K_{Ip} = (SF)\ p\ [1 + (R_i/t)]\ (\pi a)^{0.5}\ F_1 \qquad (1)$$

$$F_1 = 0.982 + 1.006(a/t)^2$$

This equation for K_{Ip} is valid for $0.20 \le a/t \le 0.50$, and includes the effect of pressure acting on the flaw faces.

For a circumferential flaw with a depth a, calculate the stress intensity factor due to internal pressure with a safety factor (SF) on pressure by using

$$K_{Ip} = (SF)\ p\ [1 + (R_i/(2t))]\ (\pi a)^{0.5}\ F_2 \qquad (2)$$

$$F_2 = 0.885 + 0.233(a/t) + 0.345(a/t)^2$$

This equation for K_{Ip} is valid for $0.20 \leq a/t \leq 0.50$, and includes the effect of pressure acting on the flaw faces.

For an axial or circumferential flaw with a depth a, calculate the stress intensity factor due to radial thermal gradients by using

$$K_{It} = ((CR)/1000)\ t^{2.5}\ F_3 \qquad (3)$$

$$F_3 = 0.584 + 2.647(a/t) - 6.294(a/t)^2 + 2.990(a/t)^3$$

This equation for K_{It} is valid for $0.20 \leq a/t \leq 0.50$, and $0 \leq (CR) \leq 100°F/hour$.

Calculate the effective flaw depth for small-scale yielding, a_e, by using

$$a_e = a + (1/(6\pi))[(K_{Ip} + K_{It})/\sigma_y]^2$$

Step 2

For an axial flaw, calculate the stress intensity factor due to internal pressure for small-scale yielding, K'_{Ip}, by substituting a_e in place of a in equation (1), including the equation for F_1. For a circumferential flaw, calculate K'_{Ip} by substituting a_e in place of a in equation (2), including the equation for F_2. For an axial or circumferential flaw, calculate the stress intensity factor due to radial thermal gradients for small-scale yielding, K'_{It}, by substituting a_e in place of a in equation (3), including the equation for F_3. Equations (1), (2) and (3) are valid for $0.20 \leq a_e/t \leq 0.50$.

The J-integral due to the applied loads for small-scale yielding is given by

$$J = 1000(K'_{Ip} + K'_{It})^2/E'$$

A-4220 EVALUATION USING CRITERION FOR FLAW GROWTH OF 0.1 IN.

Calculate the J-integral due to the applied loads, J_1, by following A-4210. Use a flaw depth a equal to $0.25t + 0.10$ in.; a pressure p equal to the accumulation pressure for Level A and B Service loadings, p_a; and a safety factor *(SF)* on pressure equal to 1.15. The acceptance criterion for Level A and B Service loadings based on a ductile flaw growth of 0.10 in. in A-2000(a)(1) is satisfied when the following inequality is satisfied.

$$J_1 < J_{0.1}$$

where J_1 = the applied J-integral for a safety factor on pressure of 1.15, and a safety factor of 1.0 on thermal loading,

$J_{0.1}$ = the J-integral resistance at a ductile flaw growth of 0.10 in.

A-4300 EVALUATION PROCEDURES FOR FLAW STABILITY

A-4310 J-R CURVE - CRACK DRIVING FORCE DIAGRAM PROCEDURE

In this procedure flaw stability is evaluated by a direct application of the flaw stability rules given in A-3400. The applied J-integral is calculated for a series of flaw depths corresponding to increasing amounts of ductile flaw growth. The applied J-integral for Level A and B Service loadings shall be calculated by using the procedures given in A-4210. The applied pressure p is set equal to the accumulation pressure for Level A and B Service loadings, p_a; and the safety factor *(SF)* on pressure is equal to 1.25. The applied J-integral is plotted against crack depth on the crack driving force diagram to produce the applied J-integral curve, as illustrated in Figure A-4310-1. The J-R curve is also plotted on the crack driving force diagram, and intersects the horizontal axis at the initial flaw depth, a_o. Flaw stability at a given applied load is demonstrated when the slope of the applied J-integral curve is less than the slope of the J-R curve at the point on the J-R curve where the two curves intersect.

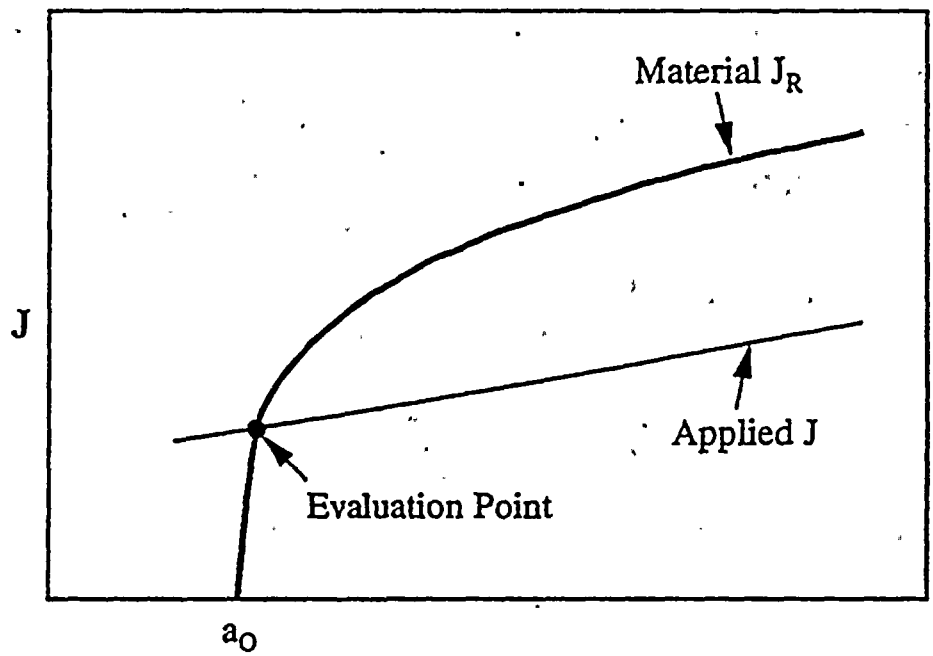

FIGURE A-4310-1 COMPARISON OF THE SLOPES OF THE APPLIED J-INTEGRAL CURVE AND THE J-R CURVE.

A-4320 FAILURE ASSESSMENT DIAGRAM PROCEDURE

This procedure is restricted to a postulated initial flaw depth equal to one-quarter of the wall thickness.

A-4321 FAILURE ASSESSMENT DIAGRAM CURVE

The same failure assessment diagram curve shall be used for axial and circumferential flaws, and is given in Figure A-4320-1. The coordinates (S_r, K_r) of the failure assessment diagram curve are given in Table A-4320-1. This curve is based on material properties which are characteristic of reactor pressure vessel steels.

A-4322 FAILURE ASSESSMENT POINT COORDINATES

The flaw depth a for a ductile flaw growth of Δa is given by

$$a = 0.25t + \Delta a$$

The failure assessment point coordinates (S_r', K_r') for a ductile flaw growth of Δa shall be calculated by using the following expressions:

$$K_r' = K_I \, [1000/(E' J_R)]^{0.5}$$

where the stress intensity factor shall be calculated using the flaw depth a without the plastic-zone correction, and is given by

$$K_I = K_{Ip} + K_{It}$$

and

$$S_r' = (SF) \, p/p_o$$

where (SF) is the required safety factor on pressure. The procedure for calculating K_{Ip}, K_{It} and p_o for axial flaws is given in A-4322.1, and for circumferential flaws in A-4322.2.

A-4322.1 Axial Flaws

The stress intensity factor due to internal pressure for axial flaws with a safety factor *(SF)* on pressure is given by equation (1). The stress intensity factor due to radial thermal gradients is given by equation (3).

The reference limit-load pressure is given by

$$p_o = \frac{(2/\sqrt{3})\,\sigma_y\,[0.905 - 0.379\,(\Delta a/t)]}{[0.379 + (R_i/t) + 0.379\,(\Delta a/t)]}$$

For materials with a yield strength σ_y greater than 85 ksi, set σ_y equal to 85 ksi in this equation. This equation for p_o is valid for $0 \le \Delta a/t \le 0.10$.

A-4322.2 Circumferential Flaws

The stress intensity factor due to internal pressure for circumferential flaws with a safety factor *(SF)* on pressure is given by equation (2). The stress intensity factor due to radial thermal gradients is given by equation (3).

The reference limit-load pressure is given by

$$p_o = \frac{\sigma_y\,[1 - 0.91\,(0.25 + (\Delta a/t))^2\,(t/R_i)]}{[1 + (R_i/(2t))]}$$

For materials with a yield strength σ_y greater than 85 ksi, set σ_y equal to 85 ksi in this equation. This equation for p_o is valid for $0 \le \Delta a/t \le 0.25$.

A-4323 EVALUATION USING CRITERION FOR FLAW STABILITY

Assessment points shall be calculated for each loading condition according to A-4322, and plotted on Figure A-4320-1 as follows. Plot a series of assessment points for various amounts of ductile flaw growth Δa up to the validity limit of the J-R curve. Use a pressure p equal to the accumulation pressure for Level A and B Service loadings, p_a; and a safety factor *(SF)* on pressure equal to 1.25. When one or more assessment points lie inside the failure assessment curve, the acceptance criterion based on flaw stability in A-2000(a)(2) is satisfied.

TABLE A-4320-1

COORDINATES OF THE FAILURE ASSESSMENT DIAGRAM CURVE OF FIGURE A-4320-1

S_r	K_r
0.000	1.000
0.050	1.000
0.100	0.999
0.150	0.998
0.200	0.996
0.250	0.993
0.300	0.990
0.350	0.987
0.400	0.981
0.450	0.973
0.500	0.960
0.550	0.939
0.600	0.908
0.650	0.864
0.700	0.807
0.750	0.737
0.800	0.660
0.850	0.581
0.900	0.505
0.950	0.435
1.000	0.374
1.050	0.321
1.100	0.276
1.150	0.238

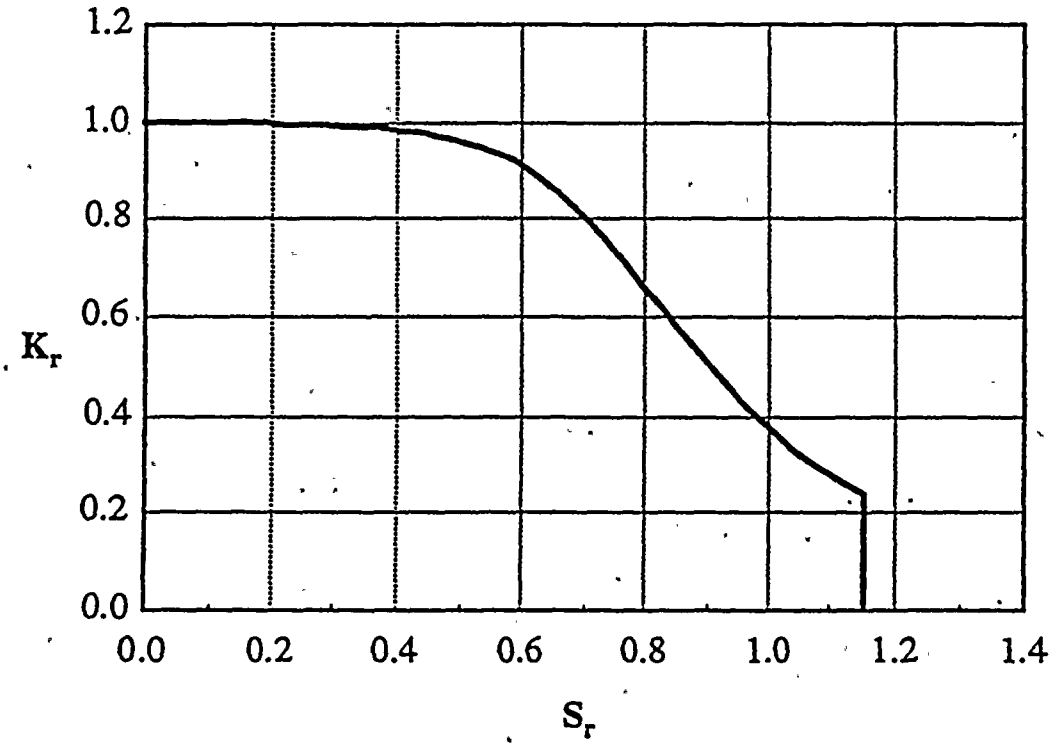

FIGURE A-4320-1 FAILURE ASSESSMENT DIAGRAM FOR THE ONE-QUARTER WALL THICKNESS FLAW.

A-4330 J-INTEGRAL/TEARING MODULUS PROCEDURE

This procedure is restricted to a postulated initial flaw depth equal to one-quarter of the wall thickness.

A-4331 J-INTEGRAL AT FLAW INSTABILITY

Referring to Figure A-4330-1, the onset of flaw instability is the point of intersection of the applied and material curves plotted on a graph of the J-integral versus tearing modulus (J versus T). The expression for the applied J/T curve is given by

$$J = (1000\ W\ t\ \sigma_f^2/E)\ T \qquad (4)$$

where σ_f is a reference flow stress which is set to 85 ksi in equation (4). For axial flaws

$$W = 0.235[1 + (0.083 \times 10^{-3})(CR)t^2/((SF)p_s)] \qquad (5)$$

where p_s is the pressure under evaluation. Equation (5) is valid for $6 \le t \le 12$ in., $2.25 \le ((SF)p_s) \le 5.00$ ksi, and $0 \le (CR) \le 100$°F/hour.

For circumferential flaws

$$W = 0.21[1 + (0.257 \times 10^{-3})(CR)t^2/((SF)p_s)] \qquad (6)$$

Equation (6) is valid for $6 \le t \le 12$ in., $2.25 \le ((SF)p_s) \le 9.00$ ksi, and $0 \le (CR) \le 100$°F/hour. Equations (4), (5) and (6) are based on material properties which are characteristic of reactor pressure vessel steels.

The tearing modulus for the material is determined by differentiation of the J-R curve with respect to flaw depth a.

$$T_R = (E/(1000\ \sigma_f^2))\ dJ_R/da \qquad (7)$$

The same values for E and σ_f shall be used in equations (4) and (7). The J-integral versus tearing modulus J_R/T_R curve for the material is given by plotting J_R against T_R for a series of increments in ductile flaw growth. Each coordinate for J_R is evaluated at the same amount of ductile flaw growth as the coordinate for T_R.

The value of the J-integral at the onset of flaw instability, J^*, corresponds to the intersection of the applied J/T curve given by equation (4) with the material J_R/T_R curve, as illustrated in Figure A-4330-1.

The J-integral at the onset of flaw instability may be determined analytically when a power-law curve fit to the J-R curve of the form

$$J_R = C_1(\Delta a)^{C_2}$$

is available. The J-integral at the onset of flaw instability, J^*, in this case is given by

$$J^* = C_1(W t C_2)^{C_2}$$

A-4332 INTERNAL PRESSURE AT FLAW INSTABILITY

The calculation of the internal pressure at the onset of flaw instability is based on the value of the J-integral at the onset of flaw instability, J^*. The ductile flaw growth at the onset of flaw instability, Δa^*, is taken from the J-R curve. The effective flaw depth at the onset of flaw instability includes the ductile flaw growth Δa^*, and is given by

$$a_e^* = 0.25t + \Delta a^* + (1/(6\pi))[J^*E'/(1000\ \sigma_y^2)]$$

The stress intensity factor due to radial thermal gradients at the onset of flaw instability, K_{It}^*, for axial or circumferential flaws is given by

$$K_{It}^* = ((CR)/1000)\ t^{2.5}\ F_3^*$$

$$F_3^* = 0.584 + 2.647(a_e^*/t) - 6.294(a_e^*/t)^2 + 2.990(a_e^*/t)^3$$

This equation for K_{It}^* is valid for $0.20 \le a_e^*/t \le 0.50$, and $0 \le (CR) \le 100$°F/hour. The stress intensity factor for small-scale yielding due to internal pressure at the onset of flaw instability, K_{Ip}^*, is given by

$$K_{Ip}^* = (J^*E'/1000)^{0.5} - K_{It}^*$$

For a given value of K^*_{Ip}, the internal pressure at the onset of flaw instability for axial flaws is given by

$$p^* = K^*_{Ip} / [(1 + (R_i/t))(\pi a^*_o)^{0.5} F^*_1]$$

$$F^*_1 = 0.982 + 1.006(a^*_o/t)^2$$

and for circumferential flaws by

$$p^* = K^*_{Ip} / [(1 + (R_i/(2t)))(\pi a^*_o)^{0.5} F^*_2]$$

$$F^*_2 = 0.885 + 0.233(a^*_o/t) + 0.345(a^*_o/t)^2$$

These equations for p^* are valid for $0.20 \leq a^*_o/t \leq 0.50$, and include the effect of pressure acting on the flaw faces.

A-4333 EVALUATION USING CRITERION FOR FLAW STABILITY

Calculate the value of the J-integral at the onset of flaw instability, J^*, by following A-4331 using a pressure p_s in equations (5) and (6) equal to the accumulation pressure for Level A and B Service loadings, p_a; and a safety factor *(SF)* on pressure equal to 1.25. Calculate the internal pressure at the onset of flaw instability, p^*, by following A-4332. The acceptance criterion based on flaw stability in A-2000(a)(2) is satisfied when the following inequality is satisfied.

$$p^* > 1.25\ p_a$$

ARTICLE A-5000

LEVEL C AND D SERVICE LOADINGS

The possible combinations of loadings and material properties which may be encountered during Level C and D Service loadings are too diverse to allow the application of pre-specified procedures and it is recommended that each situation be evaluated on an individual case basis.

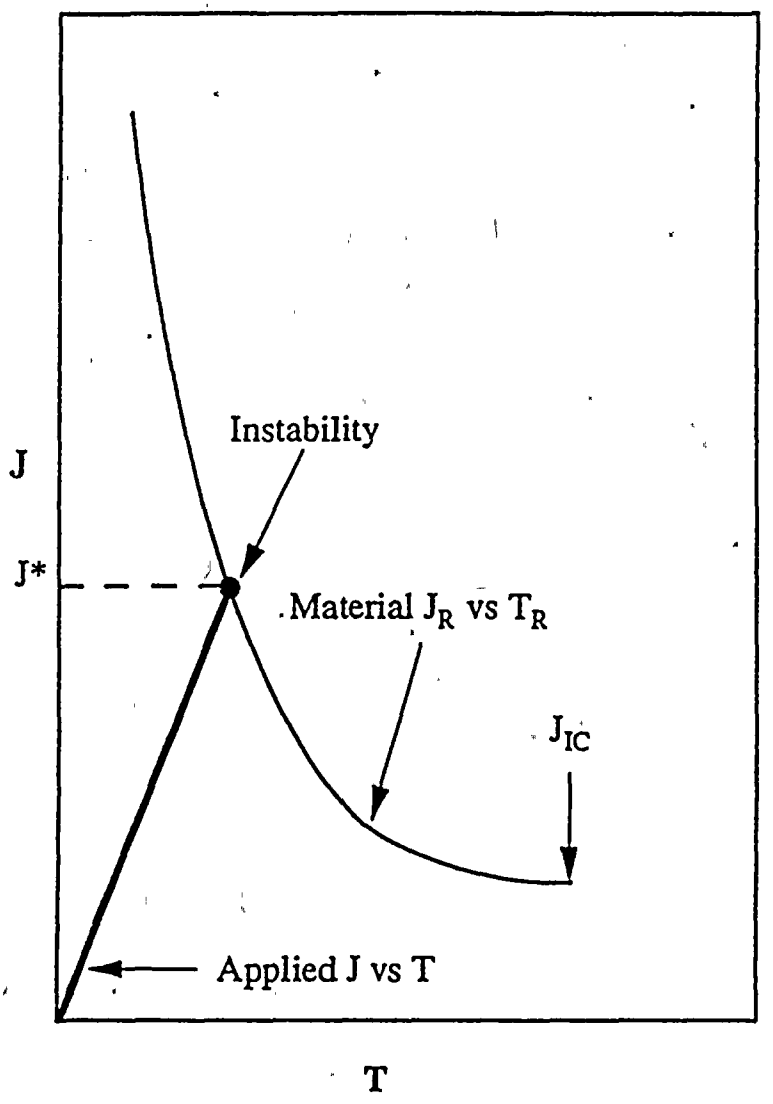

FIGURE A-4330-1 ILLUSTRATION OF THE J-INTEGRAL/TEARING MODULUS PROCEDURE

Appendix B

ASME Working Group on Flaw Evaluation

Draft Modification to Article A-3000

ARTICLE A-3000
METHOD FOR K_I DETERMINATION

"OLD TEXT"

A-3100 SCOPE

This Article provides a method for calculating stress intensity factor K_I from the membrane and bending stresses determined from stress analysis.

A-3200 STRESSES

The stresses at the flaw location should be resolved into membrane and bending stresses with respect to the wall thickness. Residual stresses and applied stresses from all forms of loading, including pressure stresses, thermal stresses, discontinuity stresses, and cladding induced stresses, should be considered. In the case of a nonlinear stress distribution through the wall, the actual stress distribution should be conservatively approximated using the linearization technique illustrated in Fig. A-3200-1. The linearized stress distribution should then be characterized by the membrane stress σ_m and the bending stress σ_b, as shown in Fig. A-3200-1.

"REPLACE WITH NEW"

A-3100 SCOPE

This Article provides a method for calculating stress intensity factor K_I from the representative stresses at the flaw location determined from stress analysis. More sophisticated techniques may be used in determining K_I provided the methods and analyses are documented.

A-3200 STRESSES

(a) For the case of a subsurface flaw, the stresses at the flaw location shall be resolved into membrane and bending stresses with respect to the wall thickness. Residual stresses and applied stresses from all forms of loading, including pressure stresses and cladding-induced stresses, shall be considered. For nonlinear stress variations through the wall, the actual stress distribution can be conservatively approximated by the linearization technique illustrated in Fig. A-3200-1(b). The linearized stress distribution should then be characterized by the membrane stress σ_m and the bending stress σ_b as shown in Fig. A-3200-1(b).

(b) For the case of a surface flaw, the stresses at the flaw location shall be represented by a polynomial fit given by the following relationship:

$$\sigma = A_0 + A_1 X + A_2 x^2 + A_3 x^3 \qquad (1)$$

where x is the distance through the wall and A_0, A_1, A_2, and A_3 are constants. The determination of coefficients A_0 through A_3 shall provide a conservative representation of stress over the crack plane $0 \le x \le a$ for all values of crack depths covered by the analysis. Stresses from sources identified in A-3200(a) shall be considered. In the case when a nonlinear stress distribution is difficult to fit be Eq. 1, the actual distribution can be conservatively approximated by the linearization technique illustrated in Figure A-3200-1(a) following the discussion given in A-3200(a) for subsurface flaws.

"OLD TEXT"

A-3300 STRESS INTENSITY EQUATION

(a) Stress intensity factors for the flaw model should be calculated from the membrane and bending stresses at the flaw location using the following equation:

$$K_I = \sigma_m M_m \sqrt{\pi} \sqrt{a/Q} + \sigma_b M_b \sqrt{\pi} \sqrt{a/Q} \quad (1)$$

where

σ_m, σ_b = membrane and bending stresses, psi, in accordance with A-3200

a = minor half-diameter, in., of embedded flaw; flaw depth for surface flaw

Q = flaw shape parameter as determined from Fig. A-3300-1 using $(\sigma_m + \sigma_b)/\sigma_y$, and the flaw geometry

M_m = correction factor for membrane stress (see Fig. A-3300-2 for subsurface flaws; Fig. A-3300-3 for surface flaws)

M_b = correction factor for bending stress (see Fig. A-3300-4 for subsurface flaws; Fig. A-3300-5 for surface flaws)

(b) Where variations in K_I around the periphery of the flaw occur, the maximum value is to be used.

(c) The use of Eq. (1) is only a recommendation for determination of K_I. More sophisticated techniques may be used, provided the methods and analyses are documented. In many cases involving complex geometries and stress distributions, the methods outlined above may be inadequate.

"REPLACE WITH NEW".

A-3300 STRESS INTENSITY FACTOR EQUATIONS

The flaw shall be represented by an ellipse that circumscribes the detected flaw as illustrated in Fig. A-3300-1. The stress intensity factors for the flaw model shall be determined from the stresses and flaw geometry as described in A-3310 for subsurface flaws and in A-3320 for surface flaws.

A-3310 Subsurface Flaw Equations

(a) Stress intensity factors for subsurface flaws shall be calculated from the membrane and bending stresses at the flaw location by the following equation:

$$K_I = [\sigma_m M_m + \sigma_b M_b] \sqrt{\pi a/Q} \quad (2)$$

where,

σ_m, σ_b = Membrane and bending stresses in accordance with A-3200(a)

a = Minor half-diameter

M_m = Correction factor for membrane stress given in Fig. A-3200-2

M_b = Correction factor for bending stress given in Fig. A-3200-3

Q = Flaw shape parameter as given by Eq. 3

The flaw shape parameter Q is calculated from the following equation:

$$Q = 1 + 4.593 (a/l)^{1.65} - q_y \quad (3)$$

where a/l is the flaw aspect ratio $0 \le a/l \le 0.5$, and q_y is the plastic zone correction factor equal to $0.212 [(\sigma_m + \sigma_b) / \sigma_y]^2$.

(b) Where variations in K_I around the periphery of the flaw occur, the maximum value is to be used in the determination of the critical flaw parameters a_c and a_f.

(c) The use of Eq. 2 is only a recommendation for determination of K_I. In some cases involving complex geometries and stress distributions, the method outlined above may not be adequate.

A-3320 *Surface Flaw Equations*

(a) Stress intensity factors for surface flaws should be calculated from the cubic polynomial stress relation by the following equation:

$$K_I = \left[A_0 G_0 + A_1 G_1 \frac{a}{} + A_2 G_2 \frac{a^2}{} + A_3 G_3 \frac{a^3}{}\right] \sqrt{\pi \frac{a}{Q}} \quad (4)$$

where,

a = Crack depth

A_0, A_1, A_2, A_3 = Coefficients from Eq. 1 that represents the stress distribution over the crack ($0 \leq x \leq a$)

G_0, G_1, G_2, G_3 = Free surface correction factors for the given stress variation provided in Tables A-3320-1 and A-3320-2 as a function of flaw aspect ratio a/ℓ, crack penetration a/t, and crack tip position (PT1 and PT2)

Q = Flaw shape parameter as given by Eq. 3 with q_y defined as

$$0.212 \left[A_0 / \sigma_{ys} \right]^2$$

(b) When the linearization method is used to convert the actual stress field into σ_m and σ_b stresses as illustrated in Fig. A-3200-1(a), then Eq. 2 shall be used to calculate K_I with the following equations for M_m, M_b, and Q:

$M_m = G_0$
$M_b = G_0 - 2\,(a/t)\,G_1$
Q = Eq. 3 where q_y is defined as $0.212 \left[(\sigma_m + \sigma_b) / \sigma_{ys} \right]^2$

(c) Where variation in K_I are the periphery of the flaw occur, the maximum value is to be used in the determination of a_s and a_t.

(d) The use of the above methods is only a recommendation for determination of K_I. In some cases involving complex geometries and stress distributions, the methods outlined above may not be adequate.

TABLE A-3300-1

INFLUENCE COEFFICIENTS FOR SURFACE FLAW AT POINT 1

		a/ℓ			
	a/t	0.0	0.1	0.2	0.5
Uniform G_0	0.0	1.122	1.112	1.094	1.040
	0.2	1.360	1.134	1.086	1.021
	0.5	2.805	1.498	1.258	1.062
	0.8	11.993	1.861	1.388	1.086
Linear G_1	0.0	0.686	0.621	0.647	0.733
	0.2	0.776	0.680	0.676	0.717
	0.5	1.317	0.807	0.736	0.733
	0.8	4.574	0.948	0.800	0.756
Quadratic G_2	0.0	0.528	0.443	0.492	0.605
	0.2	0.578	0.578	0.526	0.589
	0.5	0.876	0.583	0.556	0.597
	0.8	—	0.662	0.596	0.615
Cubic G_3	0.0	0.442	0.358	0.402	0.527
	0.2	0.476	0.431	0.442	0.513
	0.5	0.669	0.470	0.460	0.516
	0.8	—	0.522	0.488	0.530

TABLE A-3300-2

INFLUENCE COEFFICIENTS FOR SURFACE FLAW AT POINT 2

		a/ℓ			
	a/t	0.0	0.1	0.2	0.5
Uniform G_0	0.0	—	0.547	0.761	1.144
	0.2	—	0.611	0.784	1.150
	0.5	—	0.816	0.965	1.247
	0.8	—	1.262	1.283	1.400
Linear G_1	0.0	—	0.073	0.123	0.174
	0.2	—	0.080	0.127	0.200
	0.5	—	0.145	0.185	0.229
	0.8	—	0.275	0.275	0.268
Quadratic G_2	0.0	—	0.019	0.038	0.062
	0.2	—	0.023	0.044	0.075
	0.5	—	0.055	0.073	0.089
	0.8	—	0.113	0.112	0.104
Cubic G_3	0.0	—	0.006	0.017	0.034
	0.2	—	0.010	0.022	0.038
	0.5	—	0.029	0.038	0.046
	0.8	—	0.060	0.059	0.054

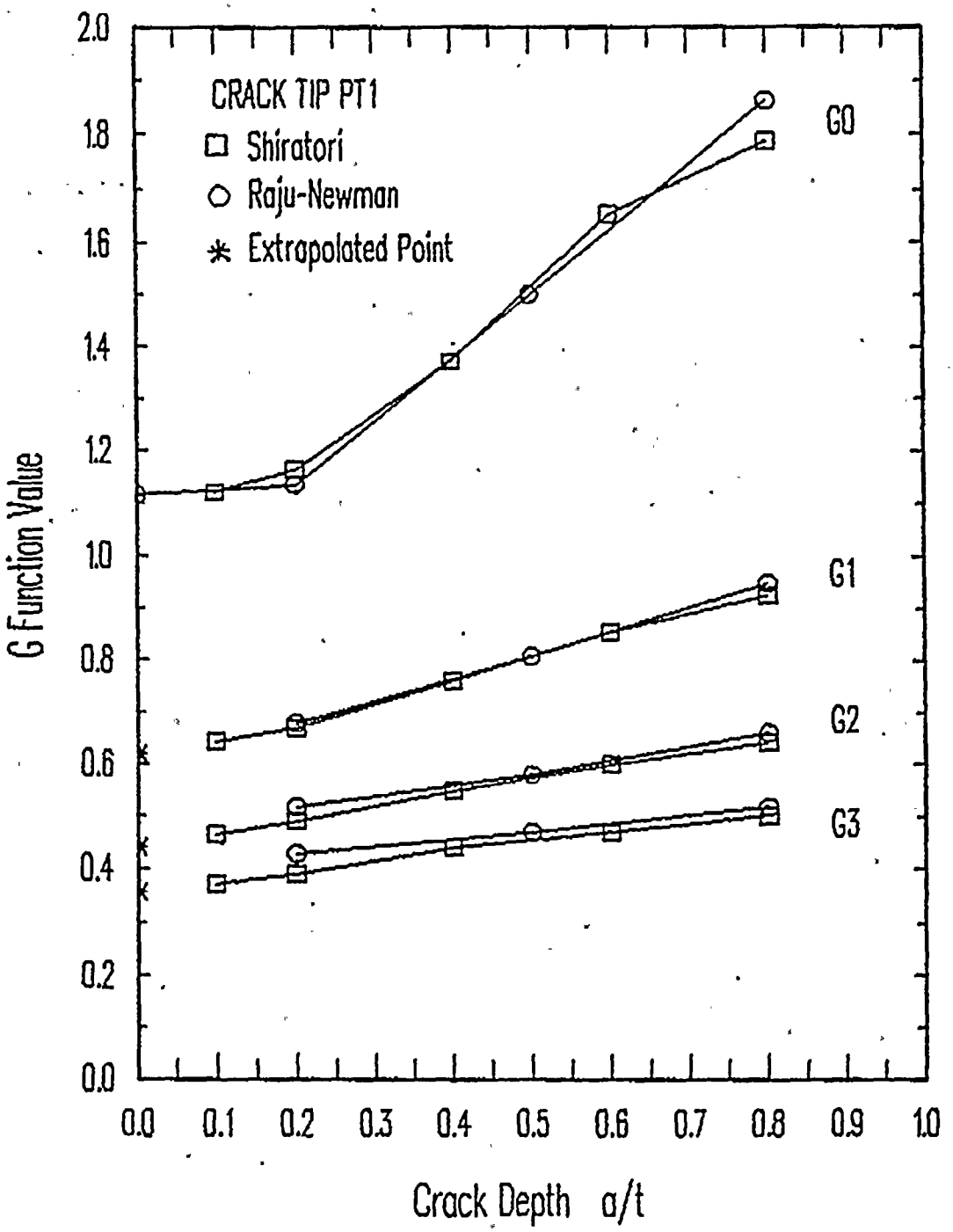
G FUNCTION RESULTS FOR A/L=0.1
CRACK TIP PT1
Shiratori
Raju-Newman
Extrapolated Point
G0
G1
G2
G3
G Function Value
Crack Depth a/t
2.0
1.8
1.6
1.4
1.2
1.0
0.8
0.6
0.4
0.2
0.0
0.0
0.1
0.2
0.3
0.4
0.5
0.6
0.7
0.8
0.9
1.0

G FUNCTION RESULTS FOR A/L=0.1

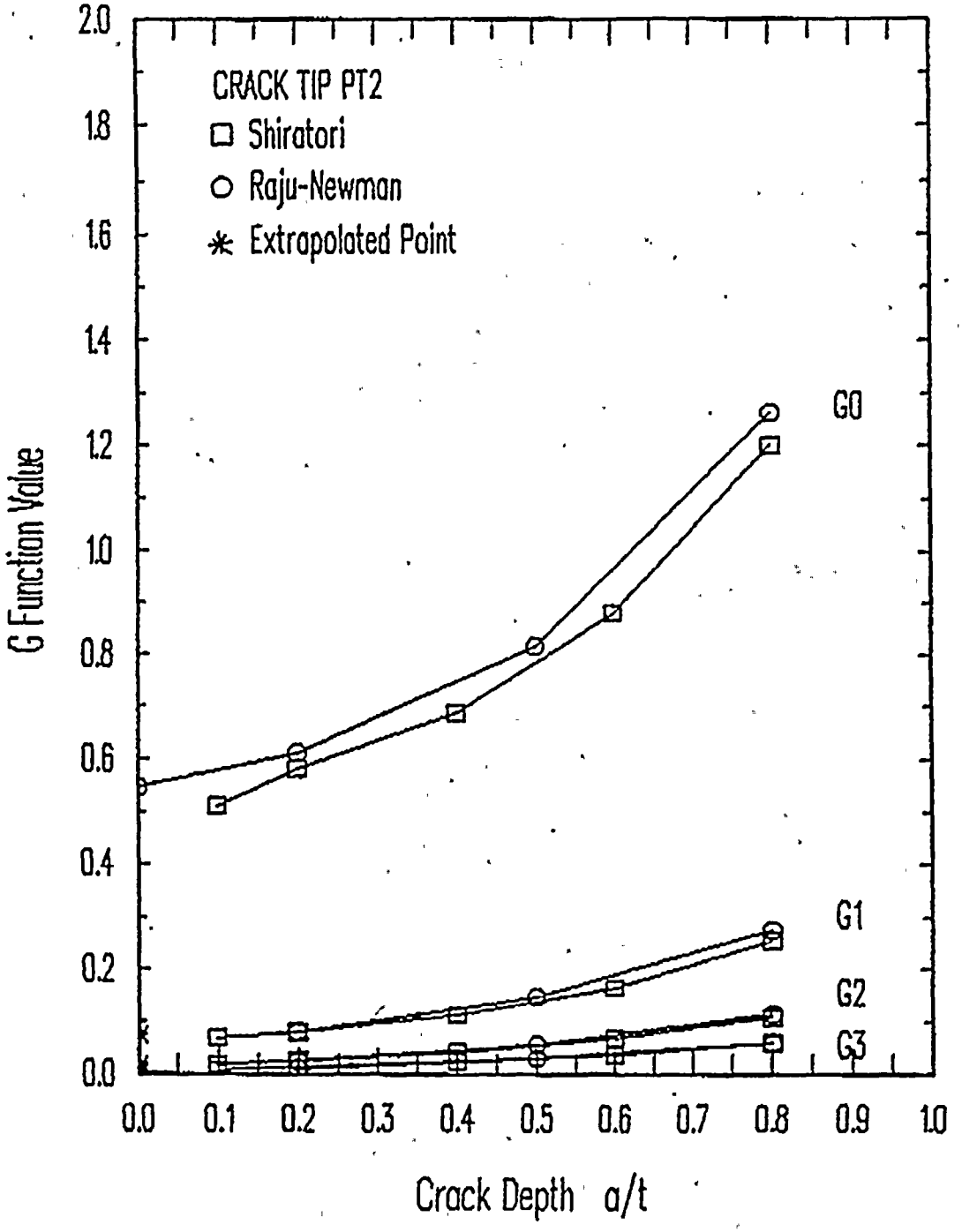

G FUNCTION RESULTS FOR A/L=0.2

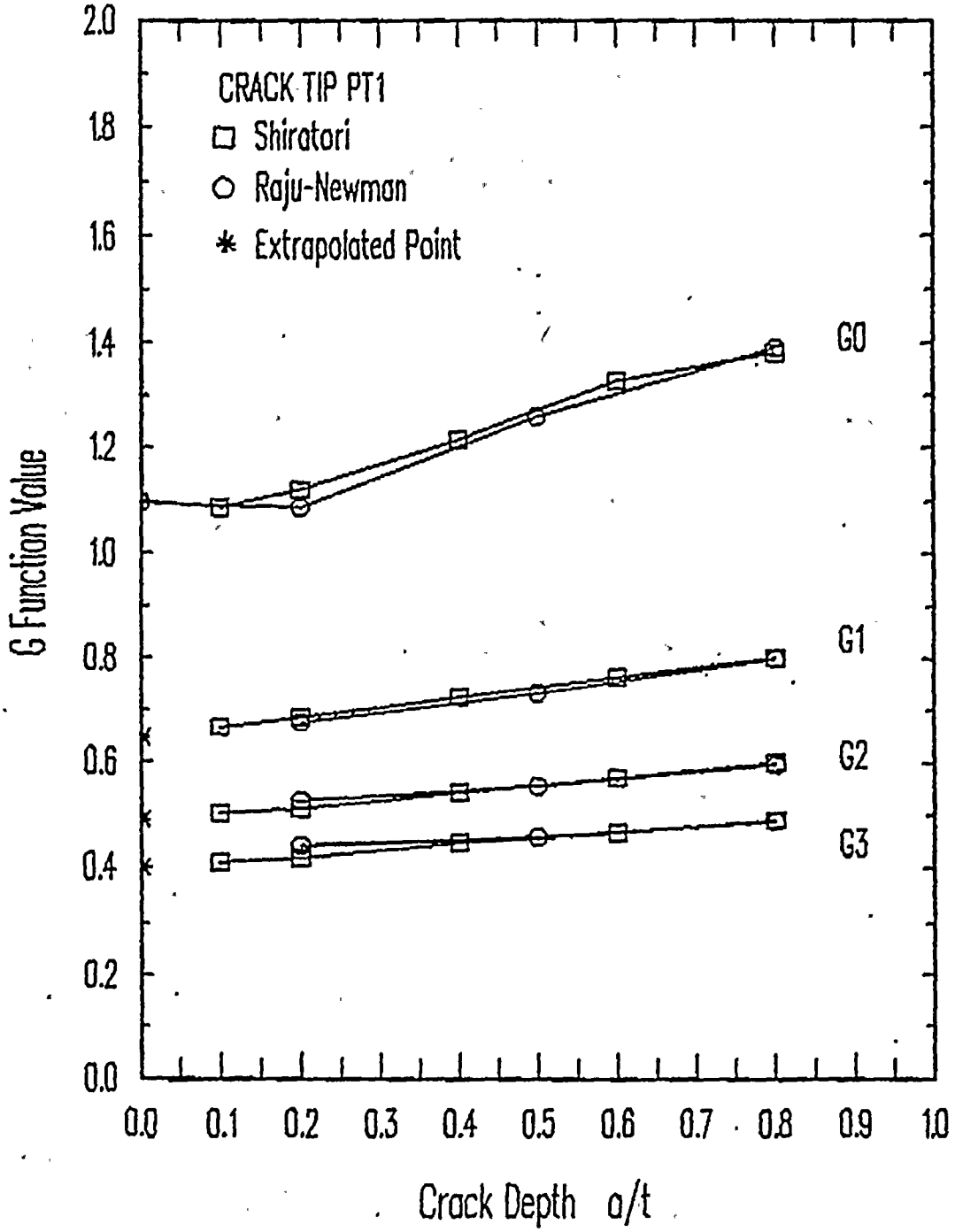

G FUNCTION RESULTS FOR A/L=0.2

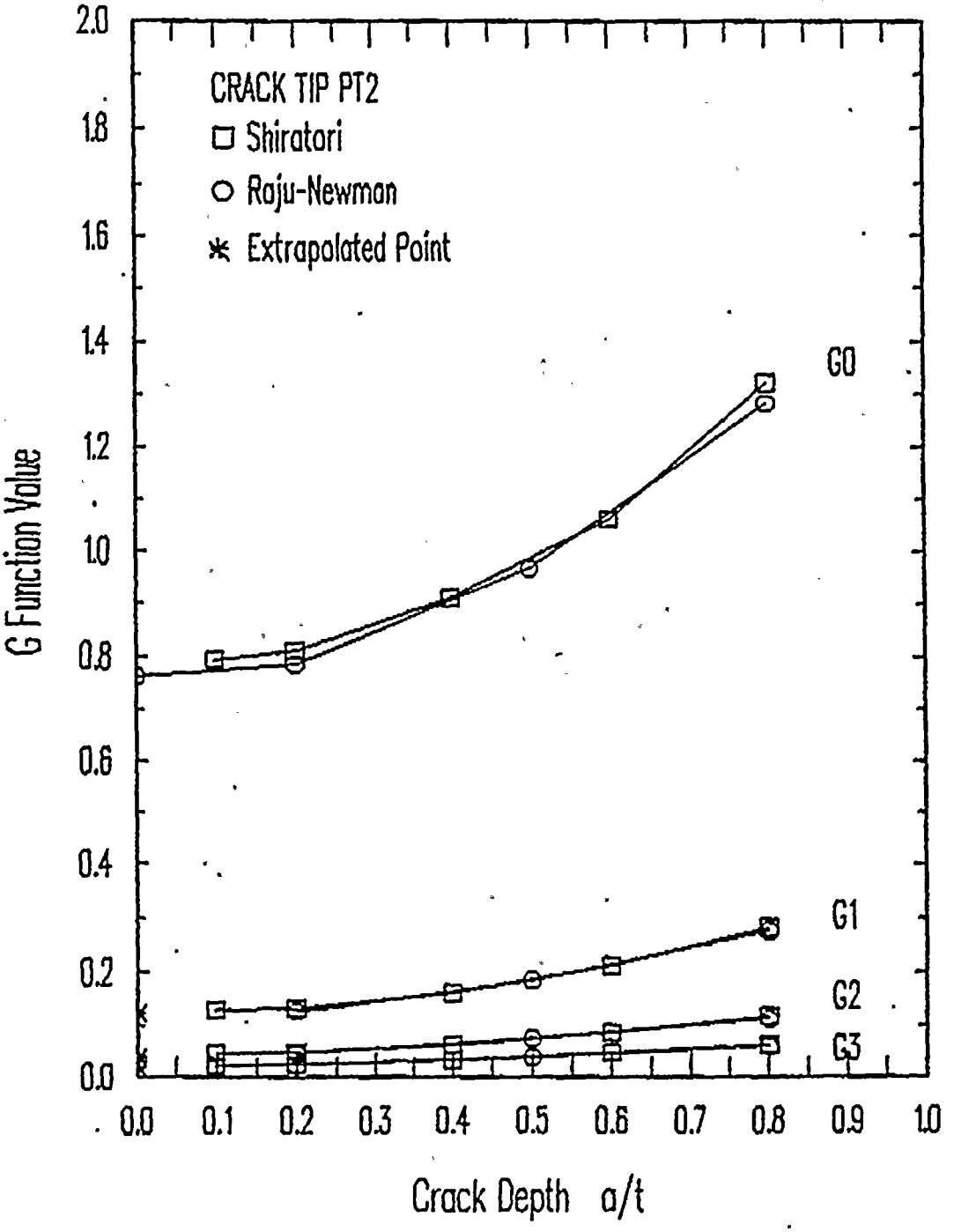

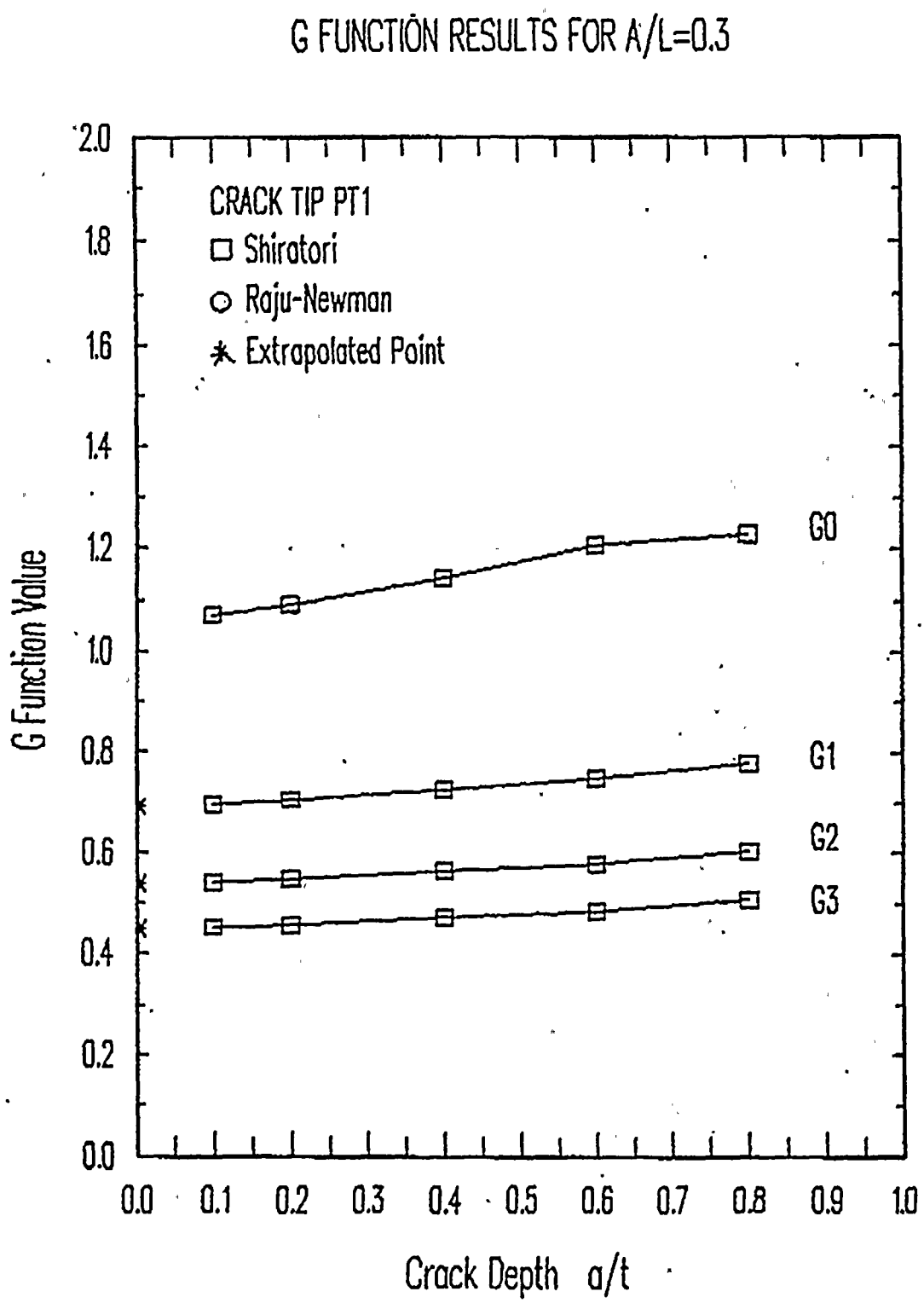
G FUNCTION RESULTS FOR A/L=0.3
CRACK TIP PT1
Shiratori
Raju-Newman
Extrapolated Point
G0
G1
G2
G3
G Function Value
Crack Depth a/t
2.0
1.8
1.6
1.4
1.2
1.0
0.8
0.6
0.4
0.2
0.0
0.0
0.1
0.2
0.3
0.4
0.5
0.6
0.7
0.8
0.9
1.0

G FUNCTION RESULTS FOR A/L=0.3

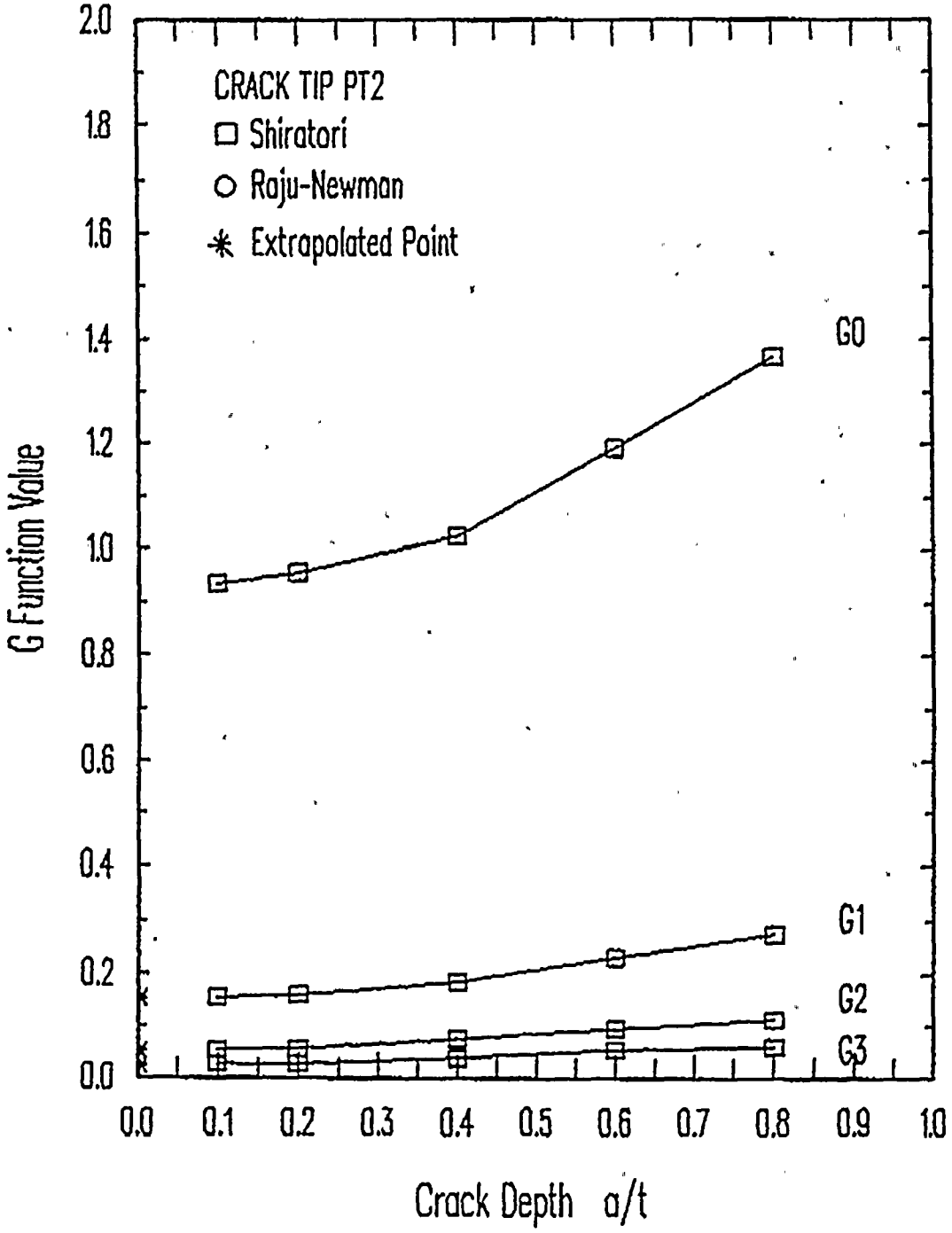

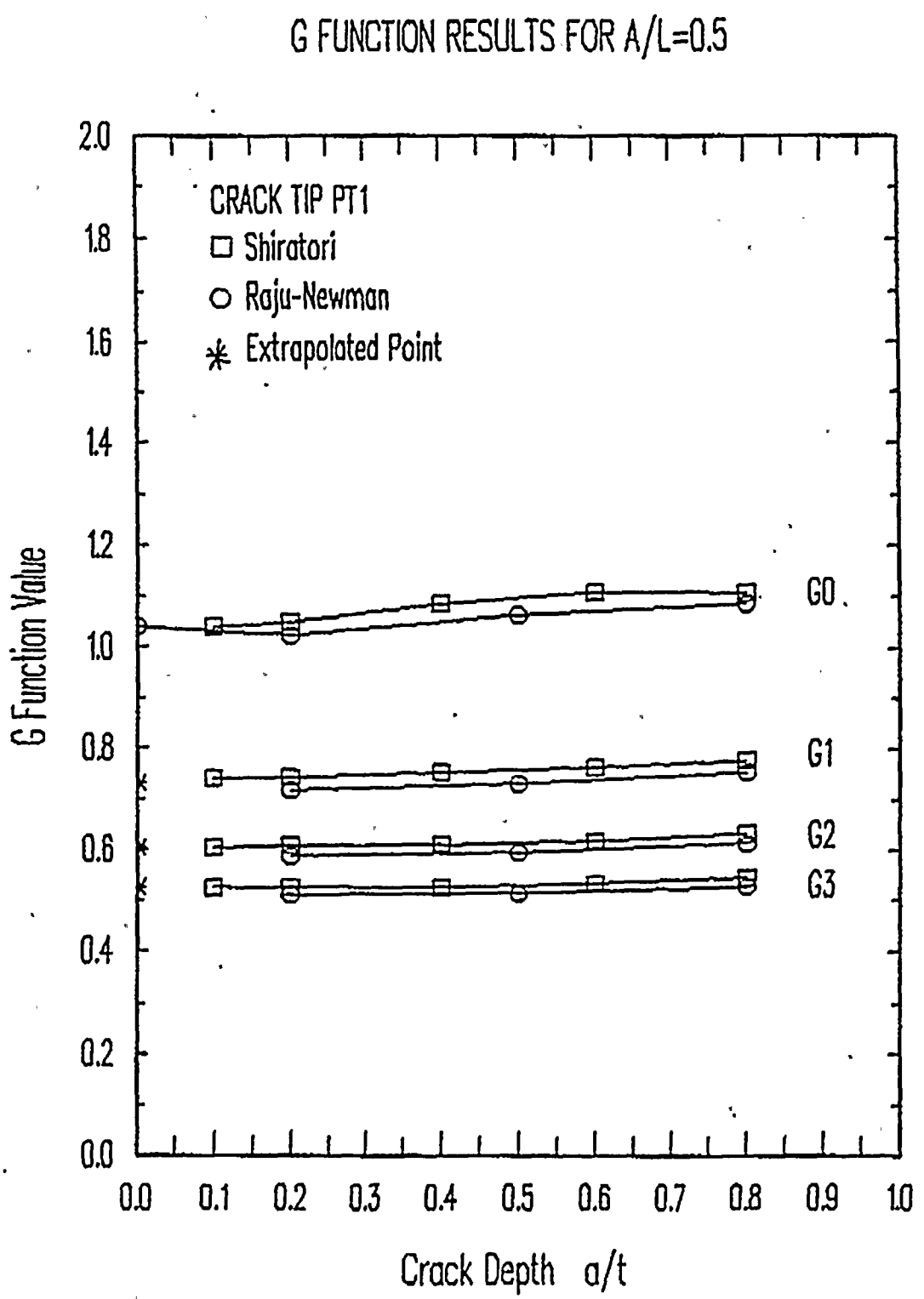
G FUNCTION RESULTS FOR A/L=0.5
CRACK TIP PT1
Shiratori
Raju-Newman
Extrapolated Point
G0
G1
G2
G3
G Function Value
Crack Depth a/t
2.0
1.8
1.6
1.4
1.2
1.0
0.8
0.6
0.4
0.2
0.0
0.0
0.1
0.2
0.3
0.4
0.5
0.6
0.7
0.8
0.9
1.0

G FUNCTION RESULTS FOR A/L=0.5

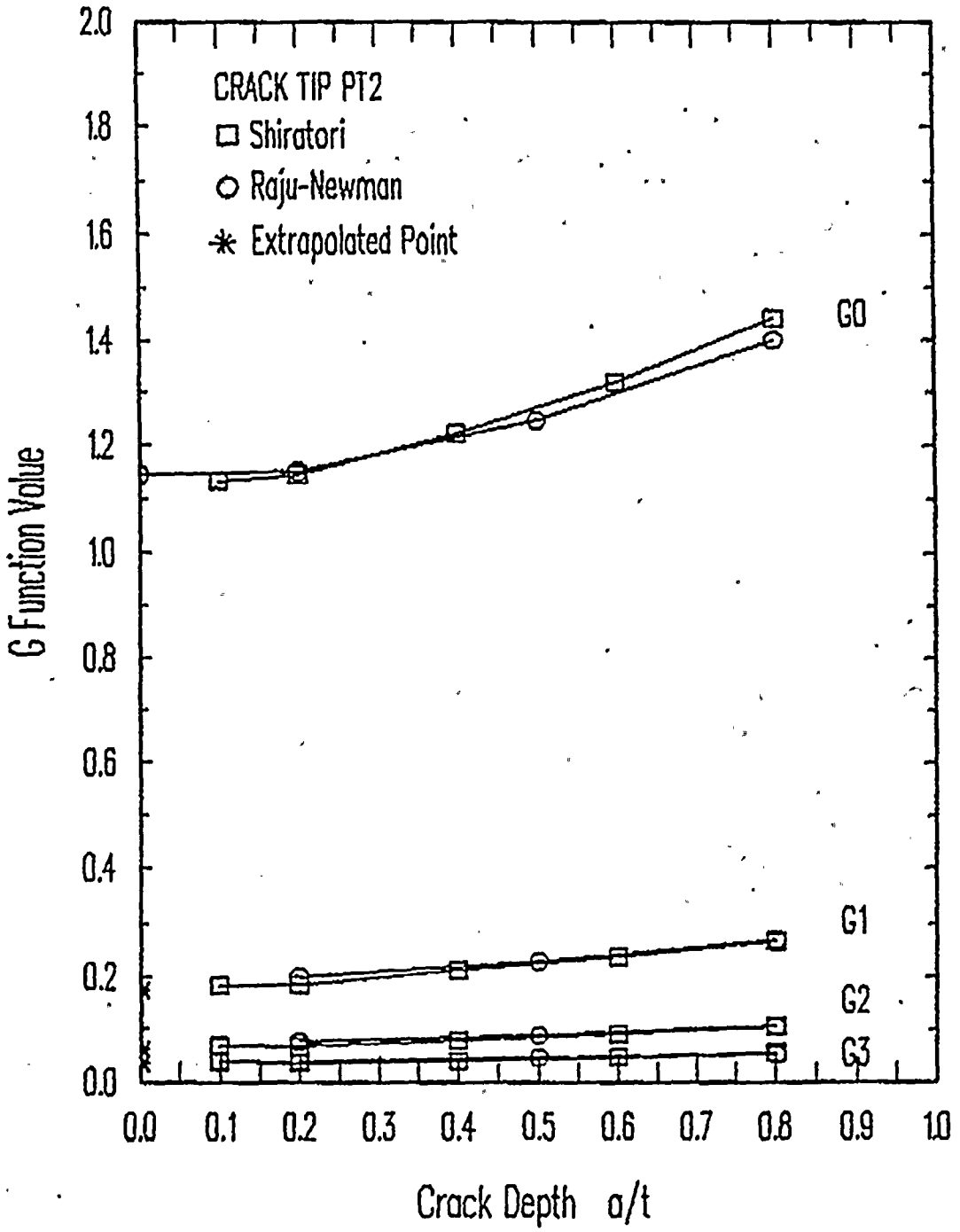

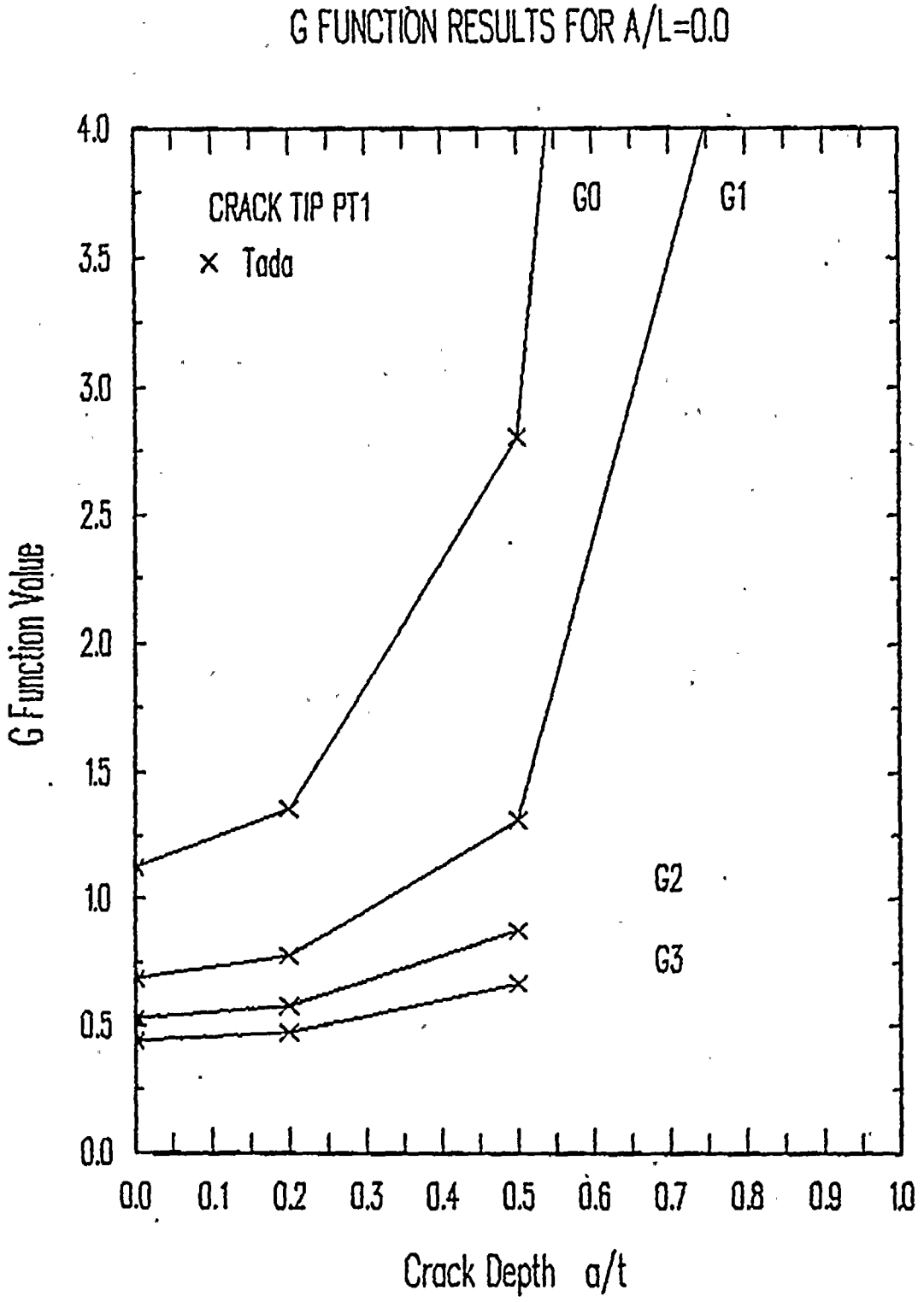
G FUNCTION RESULTS FOR A/L=0.0
CRACK TIP PT1
× Tada
G0
G1
G2
G3
G Function Value
Crack Depth a/t
4.0
3.5
3.0
2.5
2.0
1.5
1.0
0.5
0.0
0.0
0.1
0.2
0.3
0.4
0.5
0.6
0.7
0.8
0.9
1.0